Bet-hedging during bacterial diauxic shift

Ana Solopova[a], Jordi van Gestel[b], Franz J. Weissing[b,c], Herwig Bachmann[d,e], Bas Teusink[d,f], Jan Kok[a,e], and Oscar P. Kuipers[a,e,f,1]

[a]Department of Molecular Genetics, Groningen Biomolecular Sciences and Biotechnology Institute, and [b]Theoretical Biology Group, Centre for Ecological and Evolutionary Studies, University of Groningen, 9747 AG, Groningen, The Netherlands; [c]Systems Biology Centre Groningen, University of Groningen, 9713 AV, Groningen, The Netherlands; [d]Faculty of Earth and Life Sciences, Systems Bioinformatics, Centre for Integrative Bioinformatics Vrije Universiteit/ Netherlands Institute for Systems Biology, Vrije Universiteit Amsterdam, 1081 HV, Amsterdam, The Netherlands; [e]Top Institute Food and Nutrition, 6700 AN, Wageningen, The Netherlands; and [f]Kluyver Centre for Genomics of Industrial Fermentation, 2628 BC, Delft, The Netherlands

Edited* by Todd R. Klaenhammer, North Carolina State University, Raleigh, NC, and approved April 8, 2014 (received for review October 30, 2013)

When bacteria grow in a medium with two sugars, they first use the preferred sugar and only then start metabolizing the second one. After the first exponential growth phase, a short lag phase of nongrowth is observed, a period called the diauxie lag phase. It is commonly seen as a phase in which the bacteria prepare themselves to use the second sugar. Here we reveal that, in contrast to the established concept of metabolic adaptation in the lag phase, two stable cell types with alternative metabolic strategies emerge and coexist in a culture of the bacterium *Lactococcus lactis*. Only one of them continues to grow. The fraction of each metabolic phenotype depends on the level of catabolite repression and the metabolic state-dependent induction of stringent response, as well as on epigenetic cues. Furthermore, we show that the production of alternative metabolic phenotypes potentially entails a bet-hedging strategy. This study sheds new light on phenotypic heterogeneity during various lag phases occurring in microbiology and biotechnology and adjusts the generally accepted explanation of enzymatic adaptation proposed by Monod and shared by scientists for more than half a century.

phenotypic heterogeneity | Gram-positive bacteria | metabolic fitness

In nature, bacteria are confronted with a wide range of environmental conditions that change over time. These conditions often elicit specific metabolic responses that increase the division rate of a cell. For example, when bacterial cells are exposed to multiple sugars, they do not metabolize all sugars simultaneously, but rather use the sugar that allows the highest cell-division rate. Cells switch to the less-preferred sugar when the most-preferred one (in many cases glucose) is depleted. Jacques Monod coined this phenomenon "diauxie" (1). Diauxie is characterized by two growth cycles—the first one on the preferred sugar, followed by a second one on the less-preferred sugar. Both are separated by a short period during which the population apparently does not grow. This period is known as the diauxie lag phase. It is typically assumed that cells need time to make the necessary enzymatic adaptations to switch from one substrate to another (2). However, the behavior of individual cells during the lag phase has not been studied in detail. Here, we examine the diauxic shift at the single-cell level in *Lactococcus lactis* using time-lapse microscopy, in addition to the traditional approach of studying population growth characteristics. Surprisingly, the lag phase at the switch from glucose to cellobiose consumption by *L. lactis* largely results from the heterogeneous response of cells to the environmental change, rather than the time it takes for cells to make the necessary metabolic adaptations. This result challenges Monod's view of enzymatic adaptation and asks for a revision on the interpretation of population lag phases.

Results

Phenotypic Heterogeneity During Diauxie. *L. lactis* M1 is a derivative of *L. lactis* MG1363, which grows well on cellobiose because of the activation of the P*cel* promoter of the cellobiose uptake system IIC component CelB. An active cellobiose/lactose phosphotransferase system ($PTS^{Cel/Lac}$) consists of proteins PtcAB and CelB (3). A diauxic shift is seen when *L. lactis* M1 is propagated in a medium supplemented with both glucose (0.1%) and cellobiose (1%) (G-C medium; Fig. 1, green line). After a period of exponential growth, the bacterial culture stops growing at the same optical density at 600 nm (OD_{600}), which is reached when the medium only contains glucose (Fig. 1, red line). After a lag phase of no or only little population growth following the switch point, apparent population growth is resumed, eventually leading to a density that is reached when the medium only contains cellobiose (Fig. 1, blue line). In this study we mainly focus on the switch from glucose to cellobiose consumption, although diauxie is also observed in a medium with glucose and lactose (*SI Appendix*, Fig. S1).

Fig. 2*A* shows the growth of *L. lactis* M1 in G-C medium containing 1% cellobiose and a varying concentration of glucose. As expected, the switch from glucose to cellobiose utilization occurs earlier when the initial glucose concentration is lower. We visualized population growth by plotting the change in OD_{600} of a culture as the difference between two subsequent OD_{600} measurements (*SI Appendix*, Fig. S2 *B* and *D*). Interestingly, just at the switch point (arrow in Fig. 1), the OD drops; thus, the population growth value (the change in OD between two points in a growth curve) becomes negative. When we plotted this lowest population growth value for each glucose concentration (Fig. 2*B*, black dots), it appeared to be negatively correlated to the initial glucose concentration—i.e., at the switch point, the lag phase is more pronounced when cells grow initially on higher glucose concentrations. If the whole population would switch from glucose to cellobiose consumption, the opposite were to be expected—the higher the initial glucose concentration, the higher the population density would be at the switch point. This process would result in a higher population growth rate on

Significance

More than 70 years ago, Monod described the phenomenon of diauxic growth of bacteria, the observation that in the presence of two alternative sugars, cells first use one of them and then, after a short lag phase, switch to the other. Until now it had been assumed that all cells in a population engage in the outgrowth on the second sugar after major metabolic adaptation of enzymatic composition has occurred, which takes time (hence the lag phase in growth). Here, we show that actually only a subpopulation is fit enough to partake in the second growth phase and present an evolutionary model, suggesting that this phenomenon might entail a bet-hedging strategy that helps bacteria adapt to the unexpectedly changing environment.

Author contributions: A.S., H.B., B.T., J.K., and O.P.K. designed research; A.S. performed research; A.S., J.v.G., F.J.W., H.B., B.T., J.K., and O.P.K. analyzed data; and A.S., J.v.G., F.J.W., H.B., B.T., J.K., and O.P.K. wrote the paper.

The authors declare no conflict of interest.

*This Direct Submission article had a prearranged editor.

[1]To whom correspondence should be addressed. E-mail: o.p.kuipers@rug.nl.

This article contains supporting information online at www.pnas.org/lookup/suppl/doi:10.1073/pnas.1320063111/-/DCSupplemental.

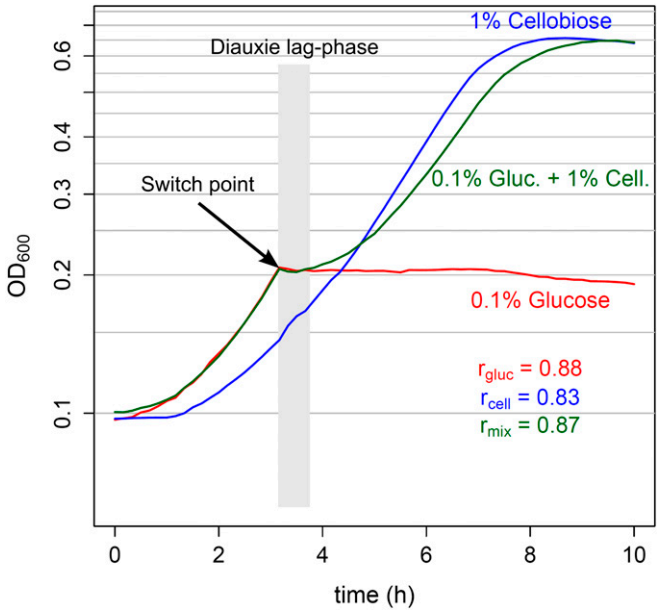

Fig. 1. *L. lactis* diauxic shift. Growth (OD_{600}) of *L. lactis* M1 in chemically defined medium with 0.1% glucose (red line), 1% cellobiose (blue line), or a mixture of 0.1% glucose and 1% cellobiose (green line) is shown; maximal growth rates (*r*) measured along the growth curves of the cultures are shown in the right lower corner. During biphasic growth in a medium with a mixture of glucose and cellobiose, cells first consume glucose. The diauxie lag phase, which follows the switch point after glucose depletion, is generally thought to result from adaptation of the metabolism of cells to using the second sugar (in this case, cellobiose). During the second exponential growth phase, cellobiose is used.

cellobiose because the population growth rate is the product of the population density and growth rate of the individual cell, given that the cellobiose concentration is very high and similar in all cases. We therefore speculated that only a fraction of the population commits to cellobiose consumption and that the size of this subpopulation depends on the glucose concentration during the first period of growth.

We investigated how many cells activate cellobiose utilization as a function of the initial glucose concentration. P*cel* is a promoter of the gene cluster *llmg_0186celB*, coding for the IIC component of the $PTS^{Cel/Lac}$. *L. lactis* M1*gfp* cells, in which P*cel* was fused to the green fluorescent protein (GFP) gene, express GFP when they take up and metabolize cellobiose. The fluorescence intensity of the culture negatively correlates with the initial glucose concentration in the medium (Fig. 2*B*, green dots): The higher the glucose concentration, the lower the intensity. Using time-lapse fluorescence microscopy, we studied the diauxic shift at the single-cell level (Fig. 2*D* and Movies S1 and S2). Cells of an isogenic population of *L. lactis* M1*gfp* growing on a mixture of glucose and cellobiose do indeed show a heterogeneous response to the change in glucose availability. At the switch point, the population differentiates into two stable phenotypes, dividing and nondividing cells. These cells are furthermore characterized by the activity of P*cel* (and the green fluorescence of GFP) being either ON or OFF, respectively. Cells in which P*cel* is ON (Cel^+ cells) express the cellobiose transporter CelB and are able to import cellobiose, use it, and grow; conversely, cells in which P*cel* is OFF (Cel^- cells) are not able to metabolize cellobiose and, consequently, do not divide. Fluorescence microscopy revealed that, in line with our earlier conclusion, the fraction of Cel^+ cells is negatively related to the initial glucose concentration in the medium (Fig. 2*C*). Although this fraction strongly reflects the initial glucose concentration (*SI Appendix*, Fig. S3), it is not affected by the initial cellobiose concentration: Even very little cellobiose (0.01%) in combination with 0.05% glucose results in the same fraction of Cel^+ cells as 1% of cellobiose with 0.05% glucose (*SI Appendix*, Fig. S4*A*). In conclusion, the microscopy results, which are confirmed by flow-cytometry data (*SI Appendix*, Fig. S4*B*), support our hypothesis that the diauxie lag phase results from a glucose concentration-dependent heterogeneous response of the population at the switch point.

The Regulation of Phenotypic Heterogeneity. How can the emergence of phenotypic heterogeneity during the diauxic shift be explained? It is well known that the order in which bacterial cells use multiple sugars depends on the global regulatory system of carbon catabolite repression (CCR) (4–7). This mechanism allows the bacteria to first consume the sugar that supports the highest growth rate (most often glucose) by shutting down expression of alternative sugar utilization pathways. The fact that the heterogeneity in *L. lactis* M1 diauxie strongly correlates with the initial glucose concentration indicates that CCR might be involved. Indeed, the P*cel* promoter region contains two binding sites (*cre* sites) for the CCR transcriptional regulator CcpA (*SI Appendix*, Fig. S5) (3). We deleted the *ccpA* gene from the chromosome of *L. lactis* M1*gfp* to examine whether population heterogeneity also occurs in the absence of CCR. The resulting strain neither shows diauxic growth in G-C medium nor exhibits population heterogeneity in the consumption of cellobiose. Instead of first consuming glucose, all cells immediately also start using cellobiose (Fig. 3; *SI Appendix*, Fig. S6; and Movie S3).

These data confirm that CCR in *L. lactis* is relieved at the switch point, after glucose is exhausted. This step then allows expression of the cellobiose gene cluster and growth of the cells on cellobiose. However, CCR is not the only factor in determining a cell's capacity to switch, and it is not the only determinant of the heterogeneity observed because, after glucose depletion and consequential relief of CCR, eventually all cells would start consuming cellobiose. In contrast, we observe two stable phenotypes: cells that have switched and use cellobiose and cells that never make the switch (Fig. 2 and Movies S1 and S2).

Expression of the cellobiose gene cluster, production and assembly of the transporter, and import of the sugar are costly and depend on the energetic state of the cell (8, 9) (*SI Appendix*, Fig. S5). The nongrowing phenotype of Cel^- cells suggests that their energetic state around the moment of glucose depletion may be too low to allow making the necessary investments in cellobiose utilization. It is important to note that the Cel^- cells are not dead—they readily divide when supplemented with glucose (Movie S4). The Cel^- cells probably remain viable because of induction of the stringent response, a protective mechanism that inhibits major energy-consuming processes in a coordinated manner as soon as bacterial cells encounter adverse conditions such as nutrient limitation or several other stresses (10). Stringent response has been observed during a lag phase in glucose–lactose diauxie of *Escherichia coli* (11) and carbon starvation in *Staphylococcus aureus* (12). The stringent response factor RelA produces the phosphorylated purine-derived alarmones (p)ppGpp in response to the presence of uncharged tRNA molecules (13–15). Stringent response depending on RelA has also been observed in *L. lactis* (16). An *L. lactis relA* knockout mutant would be expected to be unable to mount a RelA-dependent response. Postponing the stringent response might allow cells to allocate their last energy sources to the switch to cellobiose consumption. In this scenario, only those cells that are already completely energy deprived would stay Cel^-. Indeed, when *relA* was deleted from the chromosome of *L. lactis* M1*gfp*, the fraction of Cel^+ cells increased significantly for all combinations of glucose and cellobiose tested (Fig. 3, Movie S5, and *SI Appendix*, Fig. S7). The Cel^- cells remaining in a culture of *L. lactis* M1*gfp*Δ*relA* upon glucose addition resume growth, only very slowly compared with the Cel^- cells of *L. lactis* M1*gfp*. Interestingly, the fact that the *relA* mutant generates a larger fraction of Cel^+ cells than the wild-type indicates that the metabolic switch is governed by a cellular decision—namely, to induce stringent response, rather

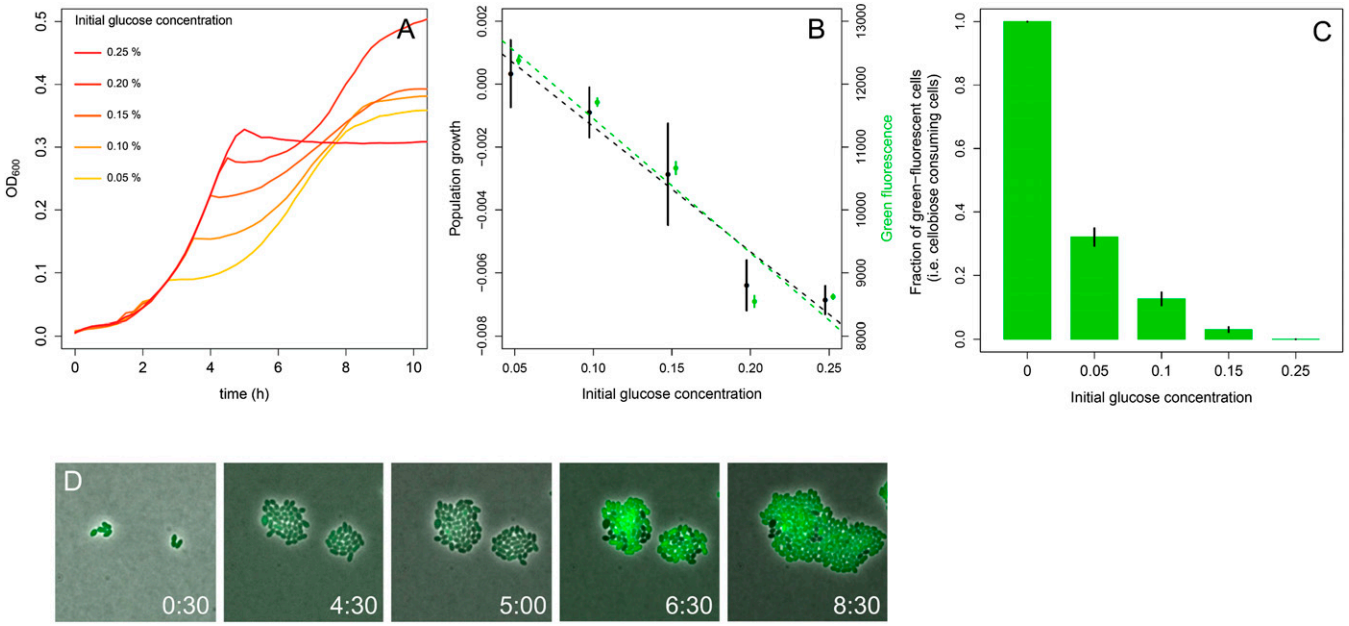

Fig. 2. Effects of initial glucose concentration on the *L. lactis* shift to growth on cellobiose. (*A*) Growth (OD_{600}) of *L. lactis* M1 in CDM, with various concentrations of glucose (0.05–0.25%; orange to red) and 1% cellobiose. (*B*) *L. lactis* M1*gfp* population growth rate expressed by the change in OD of a culture—i.e., the difference between two subsequent OD_{600} measurements (shown in *SI Appendix*, Fig. S2) (black; df = 13; $R^2 = 0.88$; $P = 2.267 \times 10^{-7}$) after the switch point is negatively related to the initial glucose concentration in the medium. The same holds for the intensity of green fluorescence of the whole population (green; df = 13; $R^2 = 0.93$; $P = 1.03 \times 10^{-8}$). Curiously, just after glucose depletion, the culture density slightly drops for all glucose–cellobiose combinations, resulting in negative values for population growth (see also *SI Appendix*, Fig. S2). Based on our microscopy data, it cannot be explained by cell lysis. This drop in culture OD is always observed at the transition point before *L. lactis* enters the stationary phase and is not a specific characteristic of diauxie. Rather, it is an intrinsic *L. lactis* property, probably attributable to cell-structure changes. However, the level of the OD drop (lowest population growth value) and the population growth rate during the second exponential growth phase correlates well with initial glucose concentration. (*C*) The fraction of cellobiose-using cells, determined on the basis of fluorescent microscopy from liquid culture samples (of identical experiments to those in *A* and *B*), also decreases with the increase of the initial glucose concentration. See also *SI Appendix*, Fig. S2. (*D*) Snapshots of the time-lapse experiment, performed in glucose and cellobiose containing CDM, illustrating appearance (at 6 h 30 min) and coexistence of two stable phenotypes: cellobiose-consuming (green cells) and nongrowing (black cells) (Movie S1). Error bars are means ± SD of three independent measurements.

than mere energy exhaustion. To further investigate the effect of the stringent response, we tested whether addition of a small amount of an energy source at the switch point could delay the response and prolong the time of cells to decide to become Cel^+. Addition of 0.01% glucose at the switch point of an *L. lactis* M1*gfp* culture growing in G-C medium indeed increases the fraction of Cel^+ cells (*SI Appendix*, Fig. S8).

In conclusion, we propose that, upon glucose depletion, *L. lactis* cells only have limited time to switch from glucose to cellobiose consumption (Fig. 4). This window in time is defined by the point at which CCR is relieved in a cell until the moment that the (p)ppGpp level gets high, and the stringent response results in a cell entering into a nongrowth state. Cel^+ cells express the cellobiose utilization system and switch to cellobiose consumption in a timely manner, replenishing their energy levels and avoiding the nongrowth state caused by the stringent response. Cel^- cells do not make this switch on time, run out of energy after glucose is completely depleted, and enter the protective nongrowing state induced by the stringent response until another carbon source that is easy to metabolize (e.g., glucose or galactose) becomes available. This hypothesis could explain why the fraction of Cel^- cells is larger for higher initial glucose concentrations. When there is more glucose in the medium, the population density at the switch point is higher and glucose depletes faster. Thus, the stringent response is triggered sooner, and, consequently, the window during which cells can switch is smaller (Figs. 2 and 4). On top of this hypothesis, accumulation or depletion of other factors in the medium could play a role in earlier induction of the stringent response when the cell density is higher.

Given that the energetic state of a cell is very important in that cell's ability to switch to another sugar, our next aim was to determine how the differences in metabolic capacity of cells arise. It is well known that *L. lactis* can activate two metabolic routes: homolactic and heterolactic fermentation. The homolactic pathway is faster but less efficient than the heterolactic pathway (less ATP molecules are produced per glucose molecule; *SI Appendix*, Fig. S5). When *L. lactis* grows on glucose, it mainly produces lactate (homolactic fermentation), whereas upon slower growth on cellobiose, it shifts to the energetically more-efficient

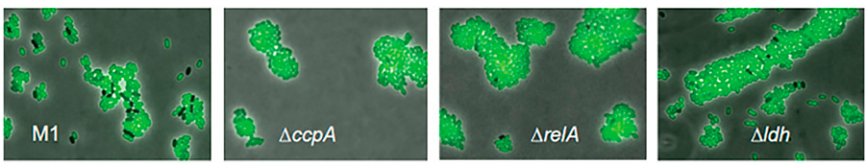

Fig. 3. Deletion of *ccpA*, *relA*, or *ldh* from the chromosome of *L. lactis* M1*gfp* increases the fraction of Cel^+ cells (green). Snapshots of time-lapse and -course experiments performed in G-C (0.1–1%) medium with different M1*gfp* deletion mutants. Overlays of phase-contrast and green fluorescence images are shown. The clumps of cells in the microscopy pictures resulted from their growth on agarose pads during time-lapse experiments and were chosen intentionally to show more cells in one picture. Neither *L. lactis* M1 nor its parent strain MG1363 forms aggregates under the conditions used in our experiments.

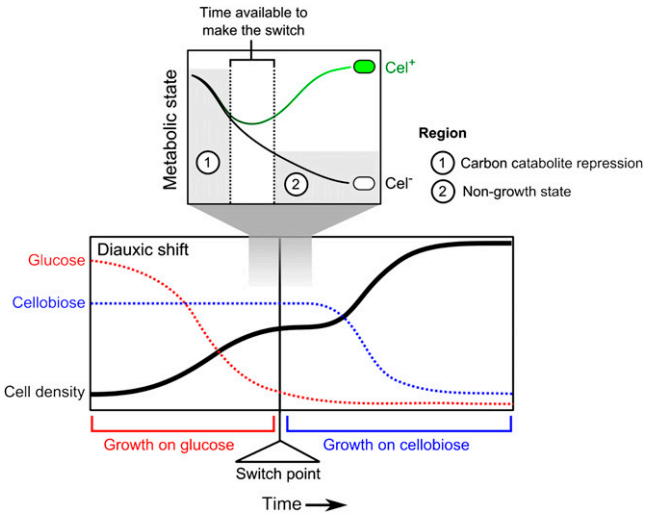

Fig. 4. Putative mechanism underlying the phenotypic heterogeneity in *L. lactis* sugar utilization. At the moment of glucose exhaustion from the medium (the switch point), the CCR level in a cell decreases. Once the repression is relieved, a cell can start expressing to the *cel* cluster and switch to cellobiose consumption, but it must have sufficient energy ("metabolic state") to do so. This switch, however, is only possible if the cell switches early enough. If the cell runs out of energy before it makes the switch, the stringent response locks the cell in a nongrowing state (Cel^-). If a cell is able to make the switch, it continues to grow using cellobiose (Cel^+).

heterolactic fermentation (17, 18). An essential enzyme in the latter pathway is acetate kinase AckA. The reaction catalyzed by this enzyme yields ATP; therefore, the expression strength of AckA can be considered as indicative of the ATP level, or metabolic fitness.

The promoter of *ackA* was shown to contain a *cre* site in *L. lactis*. Deletion of *ccpA* increased expression of the gene (7). We monitored *ackA* expression in time using the M1P*ackA-gfp* strain. At the diauxie switch the green fluorescence of individual *L. lactis* M1P*ackA–gfp* cells varies. To correlate P*ackA* expression (and ATP level) of a single cell with a Cel^+ or Cel^- phenotype, we constructed a double-labeled strain: Besides P*ackA–gfp*, we integrated a P*cel–mCherry* into the chromosome of *L. lactis* M1. Only cells with a high enough P*ackA–gfp* expression at the time of glucose exhaustion are able to switch to cellobiose consumption and become red fluorescent (activity of P*cel–mCherry*) (*SI Appendix*, Fig. S9).

Early induction of acetate kinase and the heterolactic fermentation pathway might be important in obtaining a metabolic state high enough to allow switching to cellobiose consumption, through the additional ATP gained. To test whether heterolactic fermentation plays a role in determining the fraction of Cel^+ cells, the *ldh* gene encoding the main enzyme of the homolactic fermentation pathway, lactate dehydrogenase, was deleted from the chromosome. *L. lactis* M1*gfp*Δ*ldh* only performs heterolactic fermentation and grows slower than its parent (Fig. 3 and *SI Appendix*, Fig. S10). During glucose–cellobiose diauxie, the fraction of Cel^+ cells in the *ldh* deletion strain significantly increases for all sugar combinations tested. These observations confirm that the metabolic strategy that a cell performs at the moment of glucose depletion plays an important role in the cell's ability to switch.

Epigenetics. To investigate possible preculture effects on the fraction of switching cells, we compared the diauxic growth characteristics of cells originating from glucose- or cellobiose-containing medium. *L. lactis* M1 cells from a cellobiose preculture will most likely possess several copies of the cellobiose transporter, even after a number of divisions on glucose. The presence of cellobiose transporters in a cell before the switch could facilitate sensing of and responding to cellobiose at the switch point. Our experimental data appear to confirm this hypothesis: Cells precultured in a medium with cellobiose exhibited a shorter lag phase between the two sugar utilization phases in G-C medium than those pregrown with glucose (Fig. 5 and *SI Appendix*, Fig. S2). As shown above, a shorter lag phase could be explained by a higher fraction of cells that switch to cellobiose utilization. This finding suggests the involvement of an epigenetic mechanism in metabolic switching. An epigenetic memory has been described for expression of the lactose operon *lac* of *E. coli*, which lasted for two cell generations, presumably because of expression bursts of the regulator and transporter genes involved (19).

Fig. 5 shows that preculture conditions have the strongest effect on the fraction of Cel^+ cells when the initial glucose concentration in the G-C medium is low—in other words, when only a few cell divisions are made before glucose is depleted. This finding can be explained by the fact that, during cell division, together with the membrane, a substantial fraction of the membrane proteome is being passed on to the progeny. The fewer cell divisions that occur before the change of carbon source, the more inherited cellobiose transporters that are present on the surface of a cell. To confirm this hypothesis, we placed *celB* on a plasmid under control of the nisin-inducible promoter P_{nisA} and overexpressed it in *L. lactis* M1 carrying chromosomally integrated *nisRK* to allow expression of P_{nisA}. When cells were grown in G-C medium with inducing amounts of nisin, no diauxie lag phase was observed (*SI Appendix*, Fig. S2*F*). When *celB* was overexpressed before transfer of cells to G-C medium, the diauxie lag phase became significantly shorter. This result suggests that the number of transporters produced in a cell during preculture with nisin was sufficient to support an immediate switch to cellobiose after glucose was depleted. We conclude that the destiny of a cell does not only depend on the environment of the cell but is also affected epigenetically by the environment to which the mother cell was exposed.

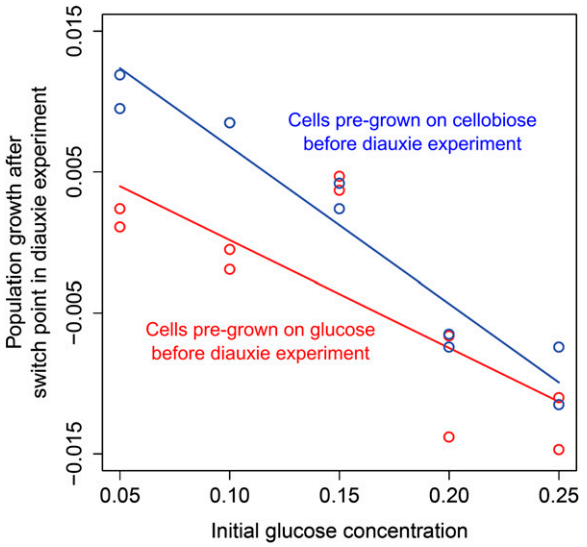

Fig. 5. Epigenetic effects influence the decision making of *L. lactis* cells. Comparison of population growth rate after the switch point for populations precultured in CDM with cellobiose (blue dots and line) and those precultured in CDM containing glucose (red dots and line) is shown. A higher fraction of cellobiose precultured cells switch to cellobiose consumption after the switch point for all initial glucose concentrations tested compared with glucose precultured cells (df = 17; $R^2 = 0.7877$; $P_{\text{initial glucose conc.}} = 9.407 \times 10^{-7}$; $P_{\text{preculture effect}} = 0.014$). See also *SI Appendix*, Fig. S2.

Heterogeneity as a Bet-Hedging Strategy. From an evolutionary perspective, the occurrence of Cel$^-$ cells seems puzzling: Why do Cel$^-$ cells not relieve CCR sooner to gain sufficient time to switch to cellobiose consumption? Might Cel$^-$ cells have a fitness benefit when supplemented with alternative sugars? To examine this possibility, we transferred a mixture of Cel$^+$ and Cel$^-$ cells to a microscopy slide containing solidified medium with galactose as the sole carbon source. Indeed, we observed that the Cel$^-$ cells divided faster than the Cel$^+$ cells on this alternate sugar (Movie S6). Apparently, there is a tradeoff: Cells that grow well on cellobiose (Cel$^+$) perform worse on galactose than Cel$^-$ cells (Fig. 6*A*). Slower growth of Cel$^+$ cells on galactose might be explained by the burden of expressing transporters and enzymes needed for cellobiose utilization, which are useless in galactose consumption.

The difference in performance of Cel$^+$ and Cel$^-$ cells on various substrates suggests that the observed population heterogeneity could be the result of adaptive evolution. A genotype that produces a mixture of Cel$^+$ and Cel$^-$ cells might have an advantage over one that produces only Cel$^+$ or only Cel$^-$ cells when future environmental conditions are unpredictable. This advantage is because the former genotype reduces the variation in fitness over time, thereby maximizing its geometric fitness (*SI Appendix*).

To examine whether such a bet-hedging strategy (20) could indeed evolve, we constructed a model based on the growth rates of Cel$^-$ and Cel$^+$ cells as derived from the time-lapse microscopy data (Movies S1, S2, and S6) and plotted the corresponding fitness landscape (Fig. 6*B*). For a variety of environments characterized by the probability P that conditions are favorable for Cel$^+$ cells (i.e., galactose influx occurs late after the switch point), it indicates the fitness of a spectrum of genotypes. Each genotype is characterized by the fraction α of cells that become Cel$^+$ following diauxie. A genotype producing a homogeneous population of Cel$^+$ cells corresponds to $\alpha = 1$; that generating only Cel$^-$ cells corresponds to $\alpha = 0$. Fig. 6*B* shows that, for most environmental conditions (i.e., for most values of P), an intermediate value of α results in the highest fitness. In other words, a heterogeneous population, corresponding to a bet-hedging strategy, has a selective advantage. As indicated by the dashed line in Fig. 6*B*, the optimal value of α (i.e., the optimal fraction of Cel$^+$ cells) increases linearly with the probability P that the environment is profitable for Cel$^+$ cells. The predictions based on the fitness landscape are in good agreement with individual-based evolutionary simulations (Fig. 6*B*; see *SI Appendix* for modeling details). It is therefore likely that the population heterogeneity described in this study—and the underlying molecular mechanisms—are the result of natural selection.

Discussion

In this study, we examined the mechanisms that underlie diauxie in *L. lactis*. During the diauxic shift from glucose to a less-preferable carbon source like cellobiose, *L. lactis* differentiates into two distinct phenotypic subpopulations. One subpopulation stops dividing, whereas the other continues to divide and grow on the second carbon source. Our findings adjust the conventional concept of diauxie lag phase. The lag phase in the population growth curve of *L. lactis* is not a result of a temporal growth arrest of the whole population, but is caused by the presence of a nongrowing subpopulation of cells in the culture.

We propose that this phenotypic heterogeneity results from the differential capacity of cells to deal with the time constraint between CCR relief needed to grow on the second sugar and the activation of the stringent response. The metabolic state of individual cells determines whether the stringent response is induced and whether they can make the switch to cellobiose consumption. The fraction of switching cells furthermore depends on epigenetic cues, such as preculture conditions.

One of the best-studied examples of heterogeneity is the *lac* operon of *E. coli.* It has been shown in the *lac* operon that artificial, nonmetabolizable inducers can trigger a heterogeneous response in the *E. coli* population (19, 21–23). In contrast to these studies, two stable alternative metabolic strategies emerge and coexist in *L. lactis* population under natural conditions of diauxie. A variation in growth rates has recently been shown to occur in an *E. coli* population during diauxic shift as a result of stochastic transcription bursts of the permease gene *lacY*, a finding that is quite different from our system (24). Stringent response and CCR have been implicated in glucose–lactose diauxie of *E. coli*, but only at the level of the whole population (11). Our study in *L. lactis* demonstrates that the outcomes of the two global regulatory processes can vary at the single-cell level, creating populations of cells that behave differently. In fact, a stochastic increase in (p)ppGpp levels in single cells has been associated with the persister phenotype in *E. coli* (25). Cells with elevated (p)ppGpp levels slowed down their metabolism via activation of toxin–antitoxin loci and became insensitive to antibiotics affecting growing cells. A microstarvation model was proposed to explain these bursts of (p)ppGpp and subsequent activation of toxin–antitoxin modules in individual cells (25). Nutrient availability varies in a culture, exposing some cells to starvation conditions that induce the stringent response. Notably, an increase in persister formation was observed when *E. coli* was subjected to a shift in carbon sources (26). In this study, the *E. coli* RelA/SpoT couple was proposed to act as a toxin/antitoxin system locking cells in a condition of stasis. *L. lactis* does not possess a SpoT analog—RelA exhibits both (p)ppGpp synthesis and degradation activities (16, 27). Nevertheless, the stringent response-induced nongrowth state of *E. coli* and that of Cel$^-$ cells of *L. lactis* appear to have similarities.

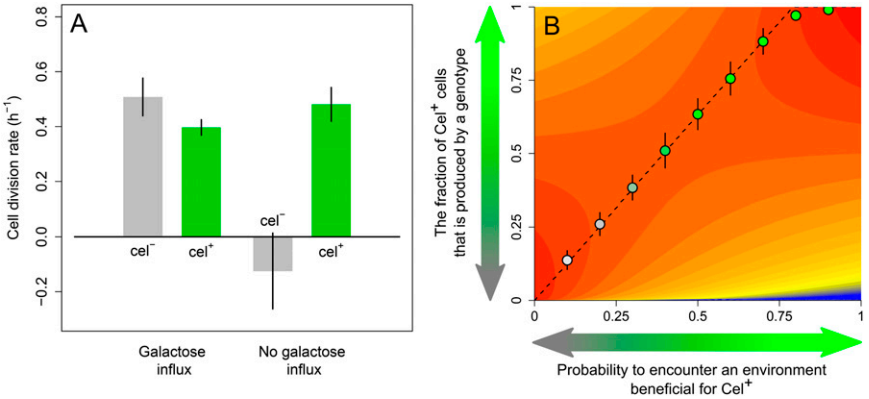

Fig. 6. Heterogeneity as a bet-hedging strategy. (*A*) Cell-division rates calculated from the time-lapse movies (Movies S1, S2, and S6) for *L. lactis* M1 Cel$^+$ and Cel$^-$ cells (n = 3). (*B*) Geometric mean fitness (blue, low; red, high) as a function of the fraction of Cel$^+$ cells produced by a genotype. The adaptive landscape shows the performance of genotypes (vertical axis) for various environmental conditions (horizontal axis) characterized by the probability P that conditions favor Cel$^+$ cells. Dotted line indicates the best-performing genotypes. All genotypes that do not exclusively produce Cel$^-$ or Cel$^+$ cells represent bet-hedging strategies. The evolved genotypes, from agent-based simulation, are superimposed on the adaptive landscape (circles, average evolved genotype; error bars, SD; n = 100; see *SI Appendix* for details).

The stringent responses in *E. coli* and *L. lactis* differ significantly with respect to their effect on central carbon metabolism (28). Instead of activating many catabolic processes—as is the case in *E. coli*—the stringent response in *L. lactis* results in the negative control of catabolism, minimizing energy use. Although ppGpp is needed for full induction of *lac* operon expression in *E. coli* (29) and stimulates the regulon of the CCR regulator Crp (11), a similar control mechanism has not been observed in Gram-positive bacteria. Differences in regulation are illustrated by the phenotype of the *relA*-deletion mutants. Although *E. coli* Δ*relA*, despite the presence of the second ppGpp synthetase SpoT, shows a prolonged lag phase during glucose–lactose diauxie (11), the lag phase in glucose–cellobiose diauxie is significantly reduced in *L. lactis* M1Δ*relA*. A comparison of the latter strain with an *E. coli relA spoT* double knockout is not possible because that strain exhibits auxotrophy for a number of amino acids and requires a specific medium in which diauxie cannot be studied (11).

Heterogeneous population responses are ubiquitous among differentiating bacteria (30–40). *L. lactis* is not known to initiate any form of differentiation—such as competence development, sporulation, or motility—that occur in many other bacteria. Here, to our knowledge, we show for the first time that heterogeneity plays a major role in the metabolism of this nondifferentiating bacterium. Furthermore, we demonstrate that the observed heterogeneity might represent a bet-hedging strategy. Application of such a strategy to nutrient transitions is previously unidentified. Even though our evolutionary model is based on the growth rates measured during the particular glucose-to-cellobiose switch studied here, it is likely that phenotypic differentiation is also beneficial for other carbon source combinations. Importantly, our work shows that many lag phases observed in microbiology and biotechnology might potentially result from heterogeneity, which contrasts the paradigm originally proposed by Monod and embraced by scientists for >70 y.

Materials and Methods

L. lactis strains were grown overnight in a chemically defined medium (CDM) supplemented with glucose or cellobiose (41). Next, they were washed with CDM and diluted 20x in fresh CDM containing cellobiose, glucose, or a mixture of both; growth and fluorescence development were monitored by using a microtiter-plate reader (Tecan Group Ltd.) or FACS (BD Biosciences). Cells for microscopy experiments were cultured in 0.1% glucose-containing CDM until they reached the midexponential growth phase; they were then washed and transferred to a microscopy slide carrying a thin layer of 1.5% (wt/vol) high-resolution agarose (Sigma-Aldrich) with G-C medium (CDM with various concentrations of glucose and 1% cellobiose). Cells were grown in a 30 °C environmental chamber and monitored with an IX71 Microscope (Olympus). Pictures were taken every 10–20 min. Experiments are described in detail in *SI Appendix*.

ACKNOWLEDGMENTS. We thank Prof. Dr. Matthias Heinemann and Dr. Jan-Willem Veening for helpful discussions and Dr. Jeroen Siebring for his advice on how to use his developed chromosomal integration system for P*ackA-gfp*. A.S. and H.B. were supported by a Stichting Technische Wetenschappen grant in the scope of Project 10619, "Understanding Preculture-Dependent Growth and Acidification Rates of *Lactococcus lactis* as the Result of Population Heterogeneity." J.v.G. is supported by the Gratama Fund and a Netherlands Organization for Scientific Research grant.

1. Monod J (1949) The growth of bacterial cultures. *Annu Rev Microbiol* 3:371–394.
2. Stanier RY (1951) Enzymatic adaptation in bacteria. *Annu Rev Microbiol* 5:35–56.
3. Solopova A, et al. (2012) A specific mutation in the promoter region of the silent *cel* cluster accounts for the appearance of lactose-utilizing *Lactococcus lactis* MG1363. *Appl Environ Microbiol* 78(16):5612–5621.
4. Loomis WF, Jr., Magasanik B (1967) Glucose-lactose diauxie in *Escherichia coli*. *J Bacteriol* 93(4):1397–1401.
5. Saier MH, Jr., et al. (1996) Catabolite repression and inducer control in Gram-positive bacteria. *Microbiology* 142(Pt 2):217–230.
6. Stülke J, Hillen W (1999) Carbon catabolite repression in bacteria. *Curr Opin Microbiol* 2(2):195–201.
7. Zomer AL, Buist G, Larsen R, Kok J, Kuipers OP (2007) Time-resolved determination of the CcpA regulon of *Lactococcus lactis* subsp. *cremoris* MG1363. *J Bacteriol* 189(4): 1366–1381.
8. Postma PW, Lengeler JW, Jacobson GR (1993) Phosphoenolpyruvate:carbohydrate phosphotransferase systems of bacteria. *Microbiol Rev* 57(3):543–594.
9. Saier MH, Jr., Reizer J (1994) The bacterial phosphotransferase system: new frontiers 30 years later. *Mol Microbiol* 13(5):755–764.
10. Chang DE, Smalley DJ, Conway T (2002) Gene expression profiling of *Escherichia coli* growth transitions: An expanded stringent response model. *Mol Microbiol* 45(2): 289–306.
11. Traxler MF, Chang DE, Conway T (2006) Guanosine 3′,5′-bispyrophosphate coordinates global gene expression during glucose-lactose diauxie in *Escherichia coli*. *Proc Natl Acad Sci USA* 103(7):2374–2379.
12. Crosse AM, Greenway DL, England RR (2000) Accumulation of ppGpp and ppGp in *Staphylococcus aureus* 8325-4 following nutrient starvation. *Lett Appl Microbiol* 31(4):332–337.
13. Cashel M (1975) Regulation of bacterial ppGpp and pppGpp. *Annu Rev Microbiol* 29: 301–318.
14. Potrykus K, Cashel M (2008) (p)ppGpp: Still magical? *Annu Rev Microbiol* 62:35–51.
15. English BP, et al. (2011) Single-molecule investigations of the stringent response machinery in living bacterial cells. *Proc Natl Acad Sci USA* 108(31):E365–E373.
16. Rallu F, Gruss A, Ehrlich SD, Maguin E (2000) Acid- and multistress-resistant mutants of *Lactococcus lactis*: Identification of intracellular stress signals. *Mol Microbiol* 35(3): 517–528.
17. Jensen NB, Melchiorsen CR, Jokumsen KV, Villadsen J (2001) Metabolic behavior of *Lactococcus lactis* MG1363 in microaerobic continuous cultivation at a low dilution rate. *Appl Environ Microbiol* 67(6):2677–2682.
18. Cocaign-Bousquet M, Even S, Lindley ND, Loubière P (2002) Anaerobic sugar catabolism in *Lactococcus lactis*: Genetic regulation and enzyme control over pathway flux. *Appl Microbiol Biotechnol* 60(1-2):24–32.
19. Robert L, et al. (2010) Pre-dispositions and epigenetic inheritance in the *Escherichia coli* lactose operon bistable switch. *Mol Syst Biol* 6:357.
20. de Jong IG, Veening JW, Kuipers OP (2012) Single cell analysis of gene expression patterns during carbon starvation in *Bacillus subtilis* reveals large phenotypic variation. *Environ Microbiol* 14(12):3110–3121.
21. Novick A, Weiner M (1957) Enzyme induction as an all-or-none phenomenon. *Proc Natl Acad Sci USA* 43(7):553–566.
22. Ozbudak EM, Thattai M, Lim HN, Shraiman BI, Van Oudenaarden A (2004) Multistability in the lactose utilization network of *Escherichia coli*. *Nature* 427(6976): 737–740.
23. Narang A, Pilyugin SS (2008) Bistability of the lac operon during growth of *Escherichia coli* on lactose and lactose+glucose. *Bull Math Biol* 70(4):1032–1064.
24. Boulineau S, et al. (2013) Single-cell dynamics reveals sustained growth during diauxic shifts. *PLoS ONE* 8(4):e61686.
25. Maisonneuve E, Castro-Camargo M, Gerdes K (2013) (p)ppGpp controls bacterial persistence by stochastic induction of toxin-antitoxin activity. *Cell* 154(5):1140–1150.
26. Amato SM, Orman MA, Brynildsen MP (2013) Metabolic control of persister formation in *Escherichia coli*. *Mol Cell* 50(4):475–487.
27. Mechold U, Cashel M, Steiner K, Gentry D, Malke H (1996) Functional analysis of a relA/spoT gene homolog from *Streptococcus equisimilis*. *J Bacteriol* 178(5): 1401–1411.
28. Dressaire C, et al. (2011) Investigation of the adaptation of *Lactococcus lactis* to isoleucine starvation integrating dynamic transcriptome and proteome information. *Microb Cell Fact* 10(Suppl 1):S18.
29. Primakoff P, Artz SW (1979) Positive control of lac operon expression in vitro by guanosine 5′-diphosphate 3′-diphosphate. *Proc Natl Acad Sci USA* 76(4):1726–1730.
30. Rao CV, Wolf DM, Arkin AP (2002) Control, exploitation and tolerance of intracellular noise. *Nature* 420(6912):231–237.
31. Elowitz MB, Levine AJ, Siggia ED, Swain PS (2002) Stochastic gene expression in a single cell. *Science* 297(5584):1183–1186.
32. Balaban NQ, Merrin J, Chait R, Kowalik L, Leibler S (2004) Bacterial persistence as a phenotypic switch. *Science* 305(5690):1622–1625.
33. Thattai M, van Oudenaarden A (2004) Stochastic gene expression in fluctuating environments. *Genetics* 167(1):523–530.
34. Kearns DB, Losick R (2005) Cell population heterogeneity during growth of *Bacillus subtilis*. *Genes Dev* 19(24):3083–3094.
35. Dubnau D, Losick R (2006) Bistability in bacteria. *Mol Microbiol* 61(3):564–572.
36. Smits WK, Kuipers OP, Veening JW (2006) Phenotypic variation in bacteria: The role of feedback regulation. *Nat Rev Microbiol* 4(4):259–271.
37. Raj A, van Oudenaarden A (2008) Nature, nurture, or chance: Stochastic gene expression and its consequences. *Cell* 135(2):216–226.
38. Veening JW, Smits WK, Kuipers OP (2008) Bistability, epigenetics, and bet-hedging in bacteria. *Annu Rev Microbiol* 62:193–210.
39. Veening JW, et al. (2008) Bet-hedging and epigenetic inheritance in bacterial cell development. *Proc Natl Acad Sci USA* 105(11):4393–4398.
40. Rainey PB, et al. (2011) The evolutionary emergence of stochastic phenotype switching in bacteria. *Microb Cell Fact* 10(Suppl 1):S14.
41. Goel A, Santos F, Vos WM, Teusink B, Molenaar D (2012) Standardized assay medium to measure *Lactococcus lactis* enzyme activities while mimicking intracellular conditions. *Appl Environ Microbiol* 78(1):134–143.

SI Materials and Methods

Microbial strains and growth conditions used

L. lactis M1 grows better on cellobiose than its parent, *L. lactis* MG1363 (1), because of the activation of the cellobiose utilization system PtcABCelB (2). *L. lactis* M1 and derivatives were grown as standing cultures at 30ºC in M17 broth (Difco™, BD, NJ, USA) or in chemically defined medium (CDM) (3) supplemented with glucose, cellobiose, lactose or galactose. When appropriate, erythromycin (Sigma – Aldrich, MO, USA) was used at 1 μg mL^{-1}. Cells for microscopy experiments were cultured in CDM with glucose or cellobiose (at 0.5% and 1% w/v, respectively) until they reached the mid-exponential growth phase, washed with CDM and transferred to a microscopy slide carrying a thin layer of 1.5% high-resolution agarose (Sigma-Aldrich) with G-C medium (CDM with various concentrations of glucose and 1% cellobiose). To test the performance of cells in a medium containing a single sugar, *L. lactis* M1*gfp* was pre-grown in G-C medium until phenotypic differentiation could be observed. Subsequently, the cells were washed, transferred to a microscopy slide carrying a 1.5% high-resolution agarose layer in CDM with glucose (1%), cellobiose (1%) or galactose (1%).

E. coli DH5α (Life Technologies, Gaithersburg, Md, USA) was used as a cloning host and was grown in tryptone yeast extract medium (Difco™) at 37°C or on tryptone yeast extract medium (both from Difco™) solidified with 1.5% (wt/vol) agar. For plasmid selection, 150 μg mL^{-1} erytromycin (Sigma-Aldrich) was added.

Microscopy

Microscopy pictures were taken with a DeltaVision (Applied Precision, Washington, USA) IX71 microscope (Olympus, PA, USA), CoolSNAP HQ2 camera (Princeton Instruments, NJ, USA),

300-W xenon light source, 100x bright field objective, GFP filter set (Chroma; excitation at 470/40 nm and emission at 525/50 nm). Snapshots were taken at 10- or 20-min intervals using 10% APLLC white LED light and a 0.05-s exposure for bright-field pictures or 100% xenon light and 0.8 sec of exposure for GFP detection. Raw data were stored using softWoRx 3.6.0 (Applied Precision) and analyzed using ImageJ (http://rsbweb.nih.gov/ij/). For the time-lapse experiments cells on a microscope slide were grown in an environmental chamber at 30°C.

Flow cytometry

Cultures were grown overnight in CDM as described above, washed and transferred to fresh CDM supplemented with various sugars and grown at 30°C. Samples were taken at 30- to 60-min intervals, and GFP levels in approximately 50,000 cells were measured with a BD FACSCanto (BD Biosciences, California, USA) flow cytometer using a 488 nm argon laser. Raw data was collected using FACSDiva Software (BD Biosciences). WinMDI 2.9 was used for data analysis (http://en.bio-soft.net/other/WinMDI.html).

Fluorescence intensity measurements

To follow fluorescence intensity changes during growth, *L. lactis* was grown at 30ºC as 200 μL cultures in 96-well microtiter plates in CDM with the appropriate sugar and monitored with an Infinite 200 PRO microtiter plate spectrophotometer (Tecan Group Ltd., Mannedorf, Switzerland). Growth was monitored by measuring the optical density at 600 nm (OD_{600}). The fluorescence intensity of GFP was monitored using excitation and emission wavelengths of 485 nm and 535 nm, respectively. For the glucose addition experiments, cells were grown as 1 mL cultures in G-C medium in 48-well microtiter plates and monitored as described above. When

the growth had reached a plateau following the switch point, glucose was added to a final concentration of 0.01% (w/v), after which growth and fluorescence were further recorded.

General DNA techniques

DNA manipulations were done essentially as described (4). Plasmid DNA and PCR products were isolated and purified using the High Pure Plasmid/PCR Isolation Kits (Roche Applied Science, Mannheim, Germany), respectively, according to the manufacturer's instructions. Restriction enzymes, T4 DNA ligase and Taq DNA-polymerase were obtained from Fermentas (Vilnius, Lithuania) and used according to the supplier's guidelines. Phusion DNA Polymerase was purchased from Finnzymes Oy (Vantaa, Finland). PCR was performed in an Eppendorf thermal cycler (Eppendorf AG, Hamburg, Germany) with *L. lactis* MG1363 chromosomal DNA as the template, using appropriate conditions.

Construction of *L. lactis* deletion strains

The PCR products obtained with primer pairs 5'-GCATTCTAGATCCATTGCGGCTTGTTGTGC-3'/5'-GCATGGATCCTCTACCATATTTGGCTATCC-3' and 5'-GCATGGATCCCATGAAATCATTTCTCGTCGCTCAAC -3'/5'-CGTACTCGAGGACCAGTCTAAAGCTGAATC-3' were cloned together as *Xba*I/*Bam*HI and *Bam*HI/*Xho*I restriction fragments (restriction sites are underlined in the sequences) in *Xba*I/*Xho*I-restricted integration vector pCS1966 (5; 6) resulting in pCS1966-*ccpA*'. The PCR products obtained with primer pairs 5'- GCATTCTAGAGAATTCGCTGGGCTTCAGTC-3'/5'-GCATGGATCCGACTGGTTCTGAAGGCATAG-3' and 5'-GCATGGATCCAAAAAAAGAGCTTGACTTAG-3'/5'-

CGTACTCGAGTGGCAAGAATCCTTGACATC-3' were cloned as *Xba*I/*Bam*HI and *Bam*HI/*Xho*I restriction fragments in *Xba*I/*Xho*I-restricted pCS1966, resulting in pCS1966-*relA*'. The PCR products of 5'- GCATTCTAGACAGCCCTTGCTGAACGTGAC-3'/5'-GCATGGATCCTTTCAACAATAGGGCCTGTC-3' and 5'-GCATGGATCCTTGCTTCTGCAGTTAAAAAC-3'/5'-CGTACTCGAGACTGCCGGGATGTTTGGAAG-3' were cloned as *Xba*I/*Bam*HI and *Bam*HI/*Xho*I restriction fragments in *Xba*I/*Xho*I-restricted pCS1966, resulting in pCS1966-*ldh*'. All pCS1966 derivatives were obtained and maintained in *E. coli* DH5α (Life Technologies). Vectors pCS1966-*ccpA*', pCS1966-*relA*' or pCS1966-*ldh*'were introduced in *L. lactis* M1*gfp* via electroporation (7); a two-step homologous recombination event was induced by growing cells on selective SA medium plates (8) supplemented with 20 μg mL^{-1} 5-fluoroorotic acid hydrate (Sigma-Aldrich). The obtained strains were checked for proper genetic make-up by sequencing (Macrogen Inc., Korea) and labeled *L. lactis* M1*gfp*Δ*ccpA*, *L. lactis* M1*gfp*Δ*relA* and *L. lactis* M1*gfp*Δ*ldh.*

Construction of CcpA, RelA and CelB overexpression strains

One copy of the nisin-inducible two-component system encoded by *nisRK* was integrated into *pepN* locus of the chromosome of M1 to allow induction by nisin.

For the overexpression of CcpA, RelA or CelB, fragments were amplified from the *L. lactis* M1 chromosome using primers 5'-CAGATCCATGGATGGTAGAATCAACAACAACAATTTATG-3'/5'-TGATATCTAGATGGGCTTAATTTTTATTTAG-3'; 5'-CAGATCCATGGATGCCTTCAGAACCAGTCTTAAC-3'/5'-TGATATCTAGAGCTCTTTTTTTAGGCATTTGTC-3' and 5'-

AGATCCATGGATGAACGGAATTACTGCGTGGATGGAG-3'/5'-GATCTCTAGATAAATCTTACCAGATTTAAC-3', respectively. The resulting PCR products were digested with *NcoI/XbaI* and cloned into the *NcoI/XbaI* sites of pNZ8048 (10) downstream of the nisin-inducible promoter P*nisA*, yielding plasmids pNZ*ccpA*, pNZ*relA* and pNZ*celB*, respectively. Expression of genes driven by P*nisA* was induced by addition of 0.1-0.5 ng/ml of nisin (Sigma-Aldrich) solution. Growth experiments of the complementation strains were performed in G-C medium. M1Δ*ccpA*, *L. lactis* M1Δ*relA* and *L. lactis* M1Δ*celB* strains possessing empty pNZ8048 vectors served as negative controls.

Construction of *gfp* and *mCherry* expression vector and strains

The P*cel* promoter fragment was amplified by PCR using primers 5'-CCGCTAGCATGCAAGCCATACTTCGTGAATAC-3'and GCATCTCGAGTAAATCTTACCAGATTTAAC-3' and ligated in pSEUDO-gfp* (2, 9) or pSEUDO-mCherry as a *SphI/XhoI* restriction fragment. Vectors, carrying P*cel-gfp* or P*cel-mCherry* were integrated in the silent locus of the chromosome of *L. lactis* M1. Excision of these vectors was performed as described previously (9), yielding *L. lactis* M1*gfp* and M1*mCherry*. The P*ackA* promoter fragment was obtained by PCR using primer pair 5'-GCATCCCGGGATCTTTATGGAAGAATTTAC-3'/5'-CGATCTCGAGTTTGGTCATGTTTAATAAAC-3'. One copy of the vector carrying P*ackA-gfp* was integrated in the chromosome of *L. lactis* M1P*mCherry*, yielding *L. lactis* M1P*ackA-gfp*P*cel-mCherry*.

Model on the evolution of bet-hedging in *L. lactis*

In order to construct a model on the evolution of bet-hedging in *L. lactis*, we determined the cell division rates of the Cel^+ and Cel^- cells when growing on cellobiose and galactose. The cell division rate could be extracted from the time-lapse microscopy experiments by getting the number of cells that is present in the first movie frame (N_0), the number of cells in the last movie frame (N_t) and the time difference between both frames (t). From these three parameters one could calculate the cell division rate in the following way:

$$r = \frac{1}{t}\log_2\left(\frac{N_t}{N_0}\right) \qquad \text{[eq. 1]}$$

Fig. 6 in the main text shows the results. As indicated before, the Cel^+ outperform the Cel^- cells when grown on cellobiose, while the opposite is found on galactose. For convenience, we annotate the Cel^- as Gal^+ cells in the rest of the model description, thereby emphasizing the trade-off between the performance of Cel^+ and Gal^+ cells on the respective substrates. The calculated cell division rates are used for all calculations that follow. Gal^+ cells are assumed to refrain from cell division on cellobiose (the negative cell division rate that is shown in Fig. 6 is based on a small fraction of Gal^+ cells that lysed just after the diauxic shift; most of them however remain viable and just refrain from growth).

Simple competition scenario

In the first version of the model we assume that cells can experience two environmental conditions: Environment A and B. In both environments we assume there are consecutive rounds

of nutrient availability: glucose → cellobiose → galactose. The time period of glucose availability is constant and the nutrient transition towards cellobiose is assumed to be a diauxic shift. Environment A and B differ in what happens after the switch point in diauxie. In environment A, cells grow for a short period (t_A) on cellobiose and are then for a long period exposed to galactose. Environment B, cells grow for a long period on cellobiose (t_B) and are then shortly exposed to galactose. A bet-hedging strategy would be a strategy that produces population heterogeneity (i.e., Cel^+ and Gal^+ cells) upon the diauxic switch from glucose to cellobiose. The timing in which cellobiose is replaced by galactose determines which cell type performs best (Gal^+ cells perform better in environment A and Cel^+ cells perform better in environment B). We assume that for each growth cycle the conditions of environment A might occur with chance *P* and that of environment B with 1-*P*. Since the whole population is exposed to the same environmental fluctuations, the fitness of a genotype is not given by the arithmetic mean cell division rate, but by the geometric mean cell division rate. It has been shown that the geometric mean can be approximated by the following equation (11-13):

$$G = \mu - \frac{\sigma^2}{2\mu} \qquad \text{[eq. 2]}$$

μ is the arithmetic mean cell division rate and σ^2 the variance in the cell division rate. The highest geometric mean does not necessarily correspond to the highest arithmetic mean, since a lower arithmetic mean cell division rate might be compensated for by less variation in the cell division rate over time. This is exactly what a bet-hedging strategy does (14-16). Since a bet-hedging genotype produces multiple cell types, there will always be cells that are not suited for the current environmental conditions as well as some that are well-adapted to it. This reduces the arithmetic mean cell division rate of this genotype compared to a pure strategy that only

expresses the well-adapted cell type. On the other hand, a bet-hedging strategy will have less variation in cell division rate over time, which increases the geometric mean cell division rate.

As a first step let us compare three strategies: one that only produces Cel^+ cells (Cel^+ pure strategy); one that only produces Gal^+ cells (Gal^+ pure strategy); and a bet-hedging strategy that produces 90% of Cel^+ and 10% of Gal^+ cells (percentages are based on time-lapse microscopy; bet-hedging strategy). If we assume that environment A and B are equally likely to occur (P=0.5) then the following table shows the arithmetic mean cell division rate, the variance and the geometric mean cell division rate of the three strategies:

Table 1. The cell division rates used for the calculations in this table are based on Fig. 6 (main text): $G_1 = 0$ (growth rate of Gal^+ cells in cellobiose); $G_2 = 0.51$ (growth rate of Gal^+ cells in galactose); $C_1 = 0.48$ (growth rate of Cel^+ cells in cellobiose); $C_2 = 0.4$ (growth rate of Cel^+ cells in galactose). In addition, we assumed that a growth cycle consisted of 25 hrs. In environment A, a galactose influx occurred after 2 hrs. (t_A) and in environment B after 23 hrs. (t_B). The cell division rates are normalized such that the highest cell division rate (that of the Cel^+ pure strategy in environment B) is equal to 1.

	Gal^+ pure strategy	Cel^+ pure strategy	Bet-hedging strategy
Environment A	0.896	0.186	0.257
Environment B	$2 \cdot 10^{-5}$	1.000	0.900
Variance (σ^2)	0.201	0.165	0.103
Arithmetic mean	0.448	0.593	0.579
Geometric mean	0.004	0.432	0.481

As explained before, the bet-hedging strategy does not have the highest arithmetic mean cell division rate (the Cel^+ pure strategy has); however the bet-hedging strategy has the lowest variation, which results in the highest geometric mean cell division rate. Since the genotype with the highest geometric mean cell division rate out-competes all others, bet-hedging is expected to evolve.

Competing the pure strategies against a set of possible bet-hedge strategies

The previous model illustrated a simple competition scenario where only one type of bet-hedging strategy was competed against two pure strategies. However, since the fraction of Gal^+ cells could be varied along a continuous scale (α), an infinite number of possible bet-hedging strategies could evolve. Only the two extreme cases of $\alpha=0$ or $\alpha=1$ correspond to pure strategies, while all other genotypes produce phenotypic heterogeneous populations (i.e., bet-hedging strategies). Moreover, also the environmental conditions to which a population is exposed could

be varied along a continuous scale P ($0 \leq P \geq 1$). We therefore addressed the following question: what is the optimal genotype (α) given the chance (P) of having a Gal$^+$-profitable environment in the future? The geometric mean cell division rate of a genotype is given by the following equation (here shown with a log-transformation):

$$\log(G) = P \cdot \log\left(\alpha \cdot N_0 \cdot e^{G_1 \cdot t_A + G_2 \cdot (T_i - t_A)} + (1-\alpha) \cdot N_0 \cdot e^{C_1 \cdot t_A + C_2 \cdot (T - t_A)}\right) +$$

[eq. 3]

$$(1-P) \cdot \log\left(\alpha \cdot N_0 \cdot e^{G_1 \cdot t_B + G_2 \cdot (T_i - t_B)} + (1-\alpha) \cdot N_0 \cdot e^{C_1 \cdot t_B + C_2 \cdot (T - t_B)}\right)$$

T is the total time period of growth on cellobiose and galactose, while t_A and t_B indicate when galactose becomes available for, respectively, environment A and B. G_1 and G_2 show the cell division rates of Gal$^+$ cells on, respectively, cellobiose and galactose. C_1 and C_2 show the cell division rates of Cel$^+$ cells on, respectively, cellobiose and galactose. N_0 shows the population size after the diauxic shift (notice that the growth period on glucose is not included in the equation, because all genotypes have the same cell division rate on glucose). The genotype with the highest geometric mean cell division rate is expected to evolve. Fig. 1 shows the geometric mean for every potential bet-hedging strategy ($0 \leq \alpha \leq 1$) for various levels of P, t_A and t_B.

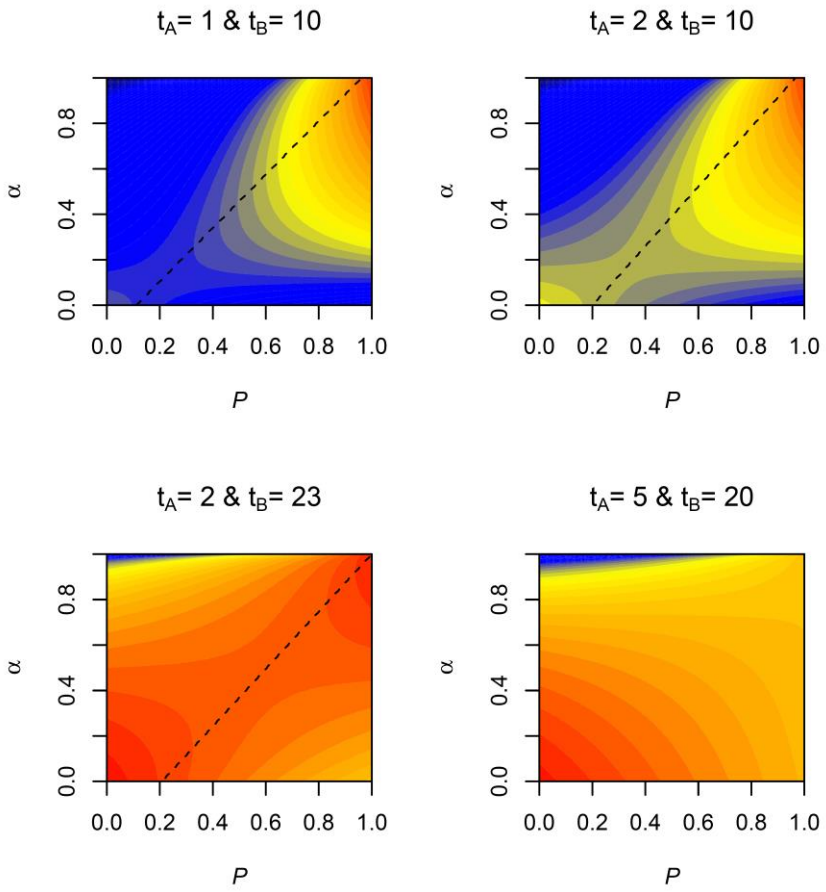

Fig. 1. Geometric mean growth rate as a function of α, *P*, t_A and t_B (T = 25). Each plot shows the adaptive landscape of a set of genotypes (α), when evolving in a particular environment (*P*). The coloration shows the geometric mean cell division rate from low (*blue*) to high (*red*). The dashed line shows the genotype (α) associated with the highest geometric mean cell division rate, given the presence of a specific *P*. In the right bottom plot there is no dashed line visible, because for all environments select for the Cel^+ pure strategy (i.e. α = 0).

Fig. 1 is based on numerical solutions of equation 3 assuming infinitely large and isogenic populations. To validate if similar results are obtained when we assume finite population sizes, which can contain mixtures of different bet-hedging strategies, we performed individual-based

simulations. In Fig. 2 we show the evolved genotypes (mean ± sd; N = 100) of our individual-based simulations, superimposed on adaptive landscape that is based on equation 3.

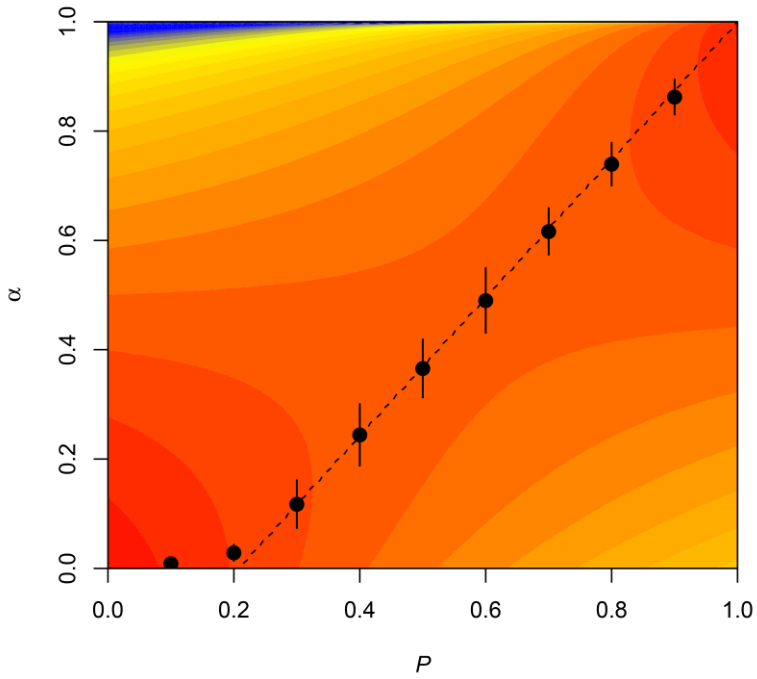

Fig. 2. Geometric mean growth rate as a function of α & *P* (*T* = 25). Here, we assume that t_1 = 2 and t_2 = 23. The coloration shows the geometric mean cell division rate from low (*blue*) to high (*red*). The *black* dots shows the average (N_{sim} = 100) evolved genotype (α), given the presence of *P*. The error bars show the associated standard deviation (notice that this plot is equal to the adaptive landscape shown in Fig. 6 (main text), with the exception that a genotype here is defined by the fraction of Gal^+ that it produces, as opposed to Cel^+). The dashed line shows the genotype (α) that is associated with the highest geometric mean cell division rate, given the presence of a specific *P*.

The individual-based simulations perfectly fit the adaptive landscape based on equation 3. Thus, in other words, for a large range of *P* values (which is an indicator of environmental fluctuations

between environment A and B over time) bet-hedging strategies evolve. Moreover, the fraction of Gal^+ cells is linearly proportional to *P* (the chance that environment A occurs), because Gal^+ cells perform best in environment A (see growth rates in Table 1). These predictions are in line with previous models on the evolution of bet-hedging (11; 12; 15; 16; 17). In conclusion, the evolved heterogeneity in *L. lactis* could potentially function as an adaptive bet-hedging strategy.

Bet-hedging in a continuous range of possible environmental changes

In the final version of the model, we will not only consider two environments that alternate over time (environment A or B), but a continuous range of environmental conditions that can occur. That is, we assume that the influx of galactose after the diauxic shift can occur at any moment in time, given a certain probability distribution. Let us assume that the influx of galactose occurs on $t = \mu_t \pm \sigma_t$ (a truncated normal distribution between time step 0 and T). In this case, the geometric mean cell division rate (log-transformed) can be given by the following equation:

$$\log(G) = \int_{t=0}^{T} \left(\frac{\frac{1}{\sigma_t \cdot \sqrt{2\pi}} \cdot e^{-\frac{1}{2}\left(\frac{t-\mu_t}{\sigma_t}\right)^2}}{P_t} \cdot \log\left(\alpha \cdot N_0 \cdot e^{G_1 t + G_2 \cdot (T-t)} + (1-\alpha) \cdot N_0 \cdot e^{C_1 t + C_2 \cdot (T-t)}\right) \right)$$

$$P_t = \int_{t=0}^{T} \frac{1}{\sigma_t \sqrt{2\pi}} e^{-\frac{1}{2}\left(\frac{t-\mu_t}{\sigma_t}\right)^2} \qquad \text{[eq. 4]}$$

Now we can again plot the geometric mean growth rate for every potential bet-hedging strategy ($0 \leq \alpha \leq 1$) for various levels of μ_t and σ_t. One would expect that bet-hedging would only evolve

when σ_t is sufficiently high, because σ_t determines the amount of environmental fluctuations over time. Furthermore, the optimal genotype (α) is expected to depend on μ_t. An environment that is associated with a small value of μ_t is better for Gal^+ cells than for Cel^+ cells, because the galactose influx appears fairly quickly after the diauxic shift. As a result, one would expect that for smaller values of μ_t the optimal genotype is associated with larger values of α. Fig. 3 shows that all results are as expected: bet-hedging would only evolve for high values of σ_t and the fraction of Gal^+ cells (α) increases for lower values of μ_t.

Thus, in short, we can conclude that the phenotypic heterogeneity that is observed in the time-lapse movies can function as a bet-hedging strategy. However, we have to make some final remarks. First, we assumed that glucose, cellobiose and galactose availability always replace each other in the same fixed order. Only the timing at which the different sugars become available varied between consecutive cycles. It might however be plausible that the order in which sugars become available varies over time as well. Further studies should therefore examine how Gal^+ and Cel^+ cells perform under various scenarios of sugar availability, to see if the same qualitative pattern would be observed when sugars would replace each other in a different order. Second, we assumed that cells can either differentiate into Gal^+ or Cel^+ cells, but it might also be possible to evolve a generalist (17). This generalist might grow slower on galactose and cellobiose than, respectively, Gal^+ and Cel^+ cells. However, it might still perform better than the bet-hedging strategy, since it also reduces the variation in growth rates over time. Finally, the model only considered three sugars and – in essence – focusses only on the presence of cellobiose and galactose. Since the observed population heterogeneity can be triggered by multiple sugars (e.g. see Fig. S1), we expect that the trade-off in cell division rates between Gal^+ and Cel^+ cells might become apparent for various other sugars as well. In this scenario, bet-

hedging could be of particular interest. It would therefore be interesting to examine if the trade-off in cell division rates, between Gal^+ and Cel^+, is present for alternative sugars.

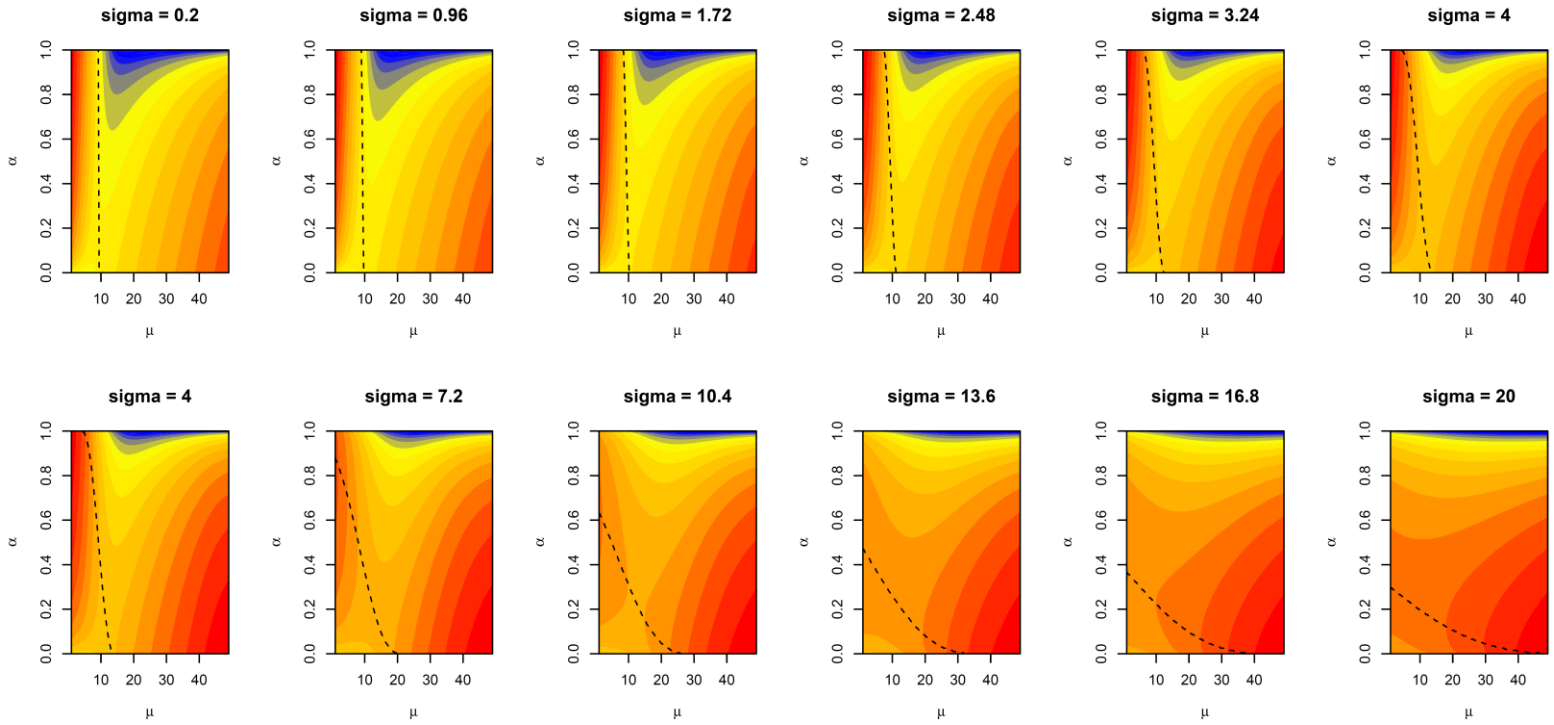

Fig. 3. Geometric mean growth rate as a function of μ_t and σ_t ($T = 50$). α is the fraction of Gal^+ cells that are produced by a genotype upon diauxie. $\mu_t \pm \sigma_t$ is the normal distribution that determines the chance of a galactose influx at time t. The background colors in each plot represent the adaptive landscape and, thereby, show the geometric mean cell division rate of a genotype. The coloration shows the geometric mean growth rate from low (*blue*) to high (*red*). The dashed line shows the genotype (α) that is associated with the highest geometric mean growth rate, given the presence of a specific selective environment (i.e. μ_t). Bet-hedging can only evolve when there is sufficient environmental variation (σ_t).

SI References

1. Gasson MJ (1983) Plasmid complements of *Streptococcus lactis* NCDO 712 and other lactic streptococci after protoplast-induced curing. *J Bacteriol* 154:1-9.
2. Solopova A, et al. (2012) A specific mutation in the promoter region of the silent *cel* cluster accounts for the appearance of lactose-utilizing *Lactococcus lactis* MG1363. *Appl Environ Microbiol* 78:5612-21.
3. Goel A, et al. (2011) Standardized assay medium to measure *Lactococcus lactis* enzyme activities while mimicking intracellular conditions. *Appl Environ Microbiol* 78:134-43.
4. Sambrook J, Fritsch EF, Maniatis T (1989) Molecular cloning: a Laboratory Manual Cold Spring Harbor (New York: Cold Spring Harbor Laboratory Press).
5. Defoor E, Kryger MB, Martinussen J (2007) The orotate transporter encoded by *oroP* from *Lactococcus lactis* is required for orotate utilization and has utility as a food-grade selectable marker. *Microbiology* 153:3645-59.
6. Solem C, Defoor E, Jensen PR, Martinussen J (2008) Plasmid pCS1966, a new selection/counterselection tool for lactic acid bacterium strain construction based on the *oroP* gene, encoding an orotate transporter from *Lactococcus lactis*. *Appl Environ Microbiol* 74:4772-5.
7. Holo H, Nes IF (1995) Transformation of *Lactococcus* by electroporation. *Methods Mol Biol* 47:195-9.
8. Jensen PR, Hammer K (1993) Minimal Requirements for Exponential Growth of *Lactococcus lactis*. *Appl Environ Microbiol* 59:4363-6.
9. Pinto JP, et al. (2011) pSEUDO, a genetic integration standard for *Lactococcus lactis*. *Appl Environ Microbiol* 77:6687-90.

10. de Ruyter PG, Kuipers OP, de Vos WM **(**1996) Controlled gene expression systems for *Lactococcus lactis* with the food-grade inducer nisin. *Appl Environ Microbiol* 62: 3662-7.

11. Frank SA, Slatkin M (1990) Evolution in a variable environment. *Amer Nat* 136:244-260.

12. Frank SA (2011) Natural selection. I. Variable environments and uncertain returns on investment. *J Evol Biol* 24:2299–2309.

13. Starrfelt J, Kokko H (2012) Bet-hedging—a triple trade-off between means, variances and correlations. *Biol Rev* 87:742-755.

14. Philippi T, Seger J (1989) Hedging one's evolutionary bets, revisited. *Trends Ecol Evol* 4:41-44.

15. Thattai M, van Oudenaarden A (2004) Stochastic gene expression in fluctuating environments. *Genetics* 167:523-30.

16. Kussell E, Leibler S (2005) Phenotypic diversity, population growth, and information in fluctuating environments. *Science* 309:2075-7.

17. Leimar O (2009) Environmental and genetic cues in the evolution of phenotypic polymorphism. *Evol Ecol* 23:125-135.

SI Figures

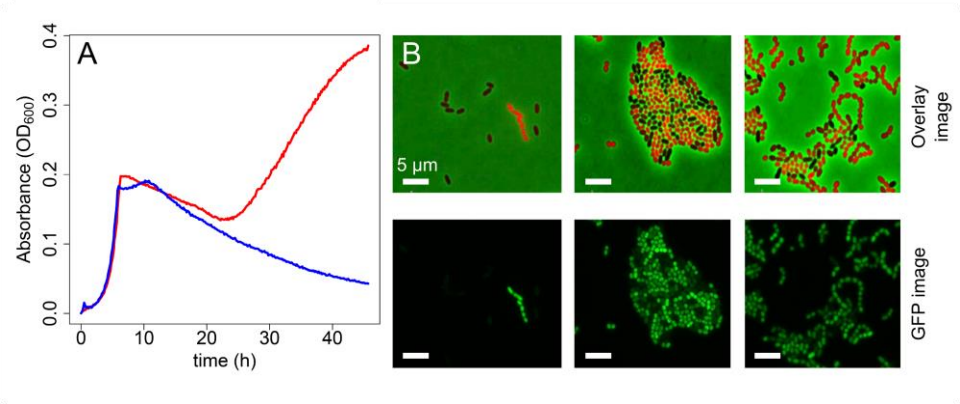

Fig. S1. Glucose-lactose diauxie exhibited by *L. lactis* M1*gfp*. (*A*) Growth (change of OD_{600} over time) of *L. lactis* M1*gfp* in a medium with 0.1% glucose and 1% lactose is biphasic (red line); blue line – growth of the same strain in a medium containing only 0.1% of glucose. Lag-phase in glucose-lactose (G-L) medium takes much longer (15 h) than in G-C medium because lactose metabolism is very slow in P-β-galactose-deficient *L. lactis* M1*gfp*. In these cells, P-β-glucosidase is used to cleave lactose-P. (*B*) Time-course microscopy images of *L. lactis* M1*gfp* growing in G-L medium, taken during the second exponential growth phase. After glucose depletion two phenotypes emerge: P*cel-gfp* expressing Lac^+ cells and non-fluorescent Lac^- cells. Lac^+ cells import lactose via the cellobiose/lactose-specific PTS PtcBACelB.

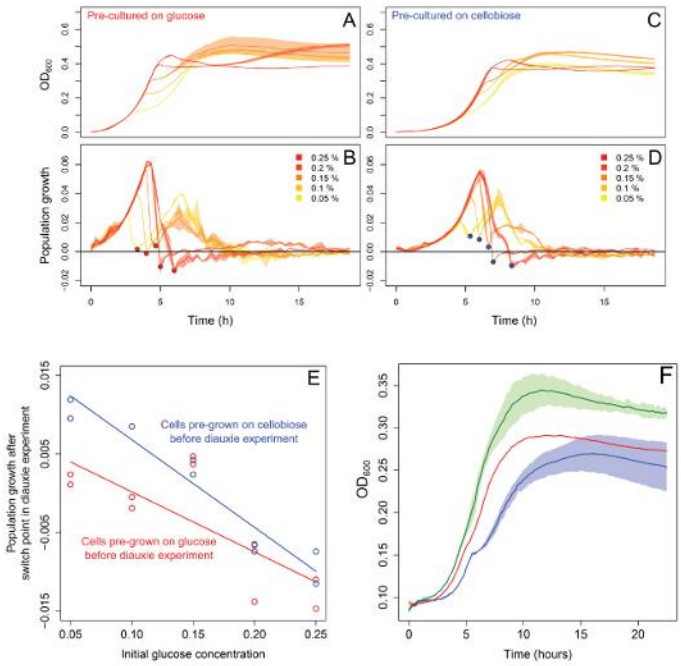

Fig. S2. The fraction of Cel$^+$ cells depends on the history of the cells. (*A*), (*B*) Growth (change of OD_{600} over time) of *L. lactis* M1*gfp* in glucose (0.05-0.25%; orange - red) - cellobiose (1%) medium. (*C*), (*D*) Population growth rate expressed by the change in optical density: difference between two subsequent OD_{600} measurements. (*A*), (*B*) Before performing the diauxie experiments, cultures were pre-grown in a glucose-containing medium (glucose pre-culture); (*C*), (*D*) Cultures originate from cellobiose pre-cultures. (*E*) Comparison of population growth after the switch point for populations pre-cultured on cellobiose (blue dots and line) and those pre-cultured on glucose (red dots and line). Higher fractions of cellobiose pre-cultured cells switch to cellobiose consumption after the switch point for all initial glucose concentrations tested, as compared to the glucose pre-grown cells in similar experiments. The differences in the growth rates correlate well with the overall fluorescence levels shown in Fig. 2*B*. This is a strong indication that pre-culture conditions indeed affect the switching behavior of cells. (*F*) Growth of *L. lactis* strains in G-C (0.1%-1%) medium: M1pNZ8048 (blue line); M1pNZ*CelB* pre-cultured in glucose-containing medium with nisin, then transferred to G-C medium without nisin (red

line); M1pNZ*CelB* pre-cultured in glucose-containing medium without nisin, then transferred to G-C medium with nisin (green line). Overexpression of cellobiose transporter IIC component CelB prior to exposure to diauxie conditions (G-C medium) significantly reduces diauxie lag-phase (red line). Expression of CelB transporters throughout the growth in G-C medium abolishes the diauxie lag-phase (green line). The growth curves show mean and sd (shaded part) for N=2. The correlation plots: df = 17; $P_{\text{glucose concentration}} = 9.4*10^{-7}$; $P_{\text{pre-culture effect}} = 0.014$; $R^2=0.79$.

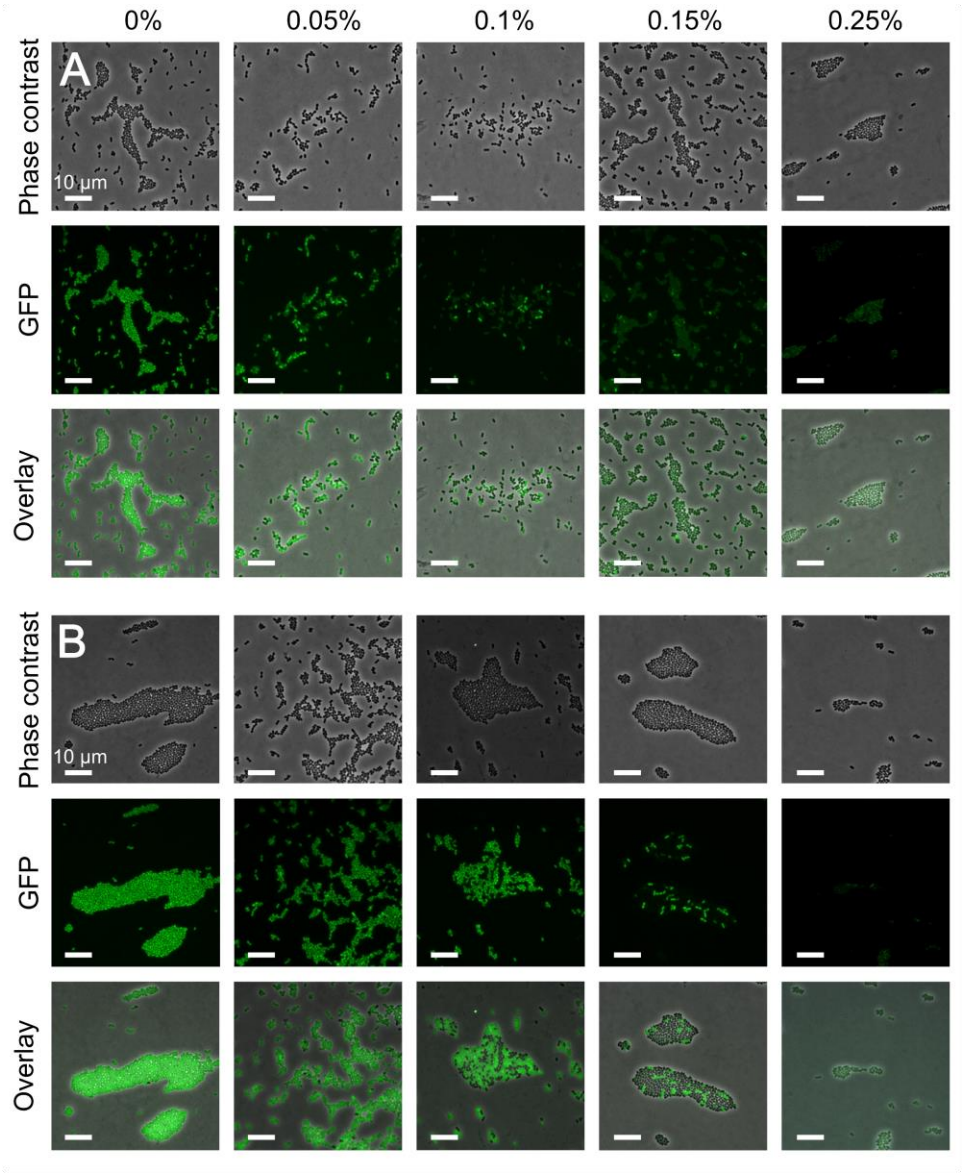

Fig. S3. The fraction of *L. lactis* M1*gfp* Cel$^+$ cells depends on the glucose concentration in G-C medium. The percentage of glucose in the medium is indicated at the top of the figure, cellobiose was present at 1%. (*A*) Microscopy images taken immediately after the switch point. Phase contrast, green fluorescence (GFP) images and their overlays are shown. (*B*) Microscopy images (phase contrast, green fluorescence (GFP) and overlays) of the same cultures taken in the stationary phase.

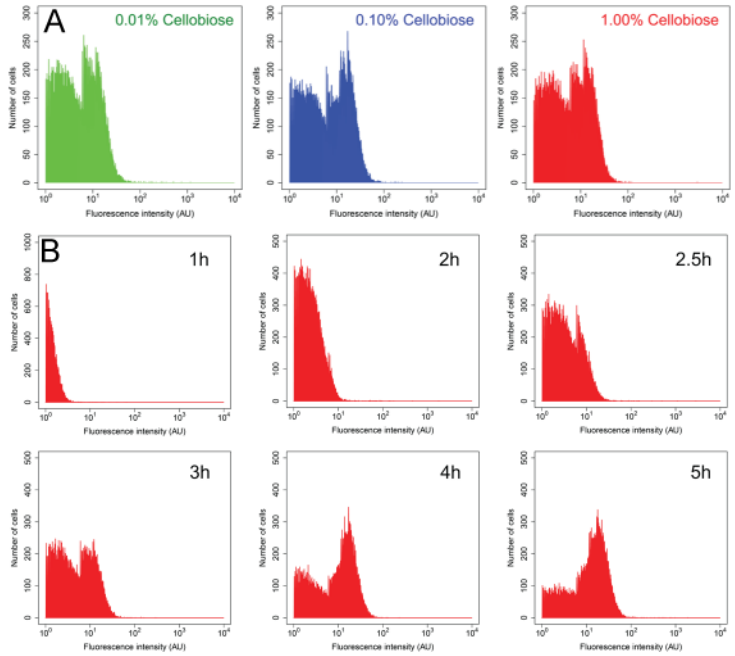

Fig. S4. Phenotypic heterogeneity in a population of *L. lactis* M1. (*A*) The fraction of *L. lactis* M1*gfp* Cel$^+$ cells does not correlate with the initial cellobiose concentration in the medium: independent of the cellobiose concentration (0.01%, 0.1% or 1%) in combination with a constant glucose concentration (0.1%) a similar fraction of cells become Cel$^+$. The two major peaks correspond to non-fluorescent (left-side of each histogram) and fluorescent (right-side of each histogram) cell subpopulations. The heights of the respective peaks show the relative sizes of subpopulations. (*B*) Phenotypic differentiation of an isogenic *L. lactis* M1*gfp* population into two subpopulations during diauxie. Flow cytometry data shows that in a G-C (1%-0.05%) medium, after glucose is exhausted, a GFP-expressing cellobiose-consuming subpopulation emerges (2.5h) and increases in size. A fraction of cells remain Cel$^-$ (non-fluorescent subpopulation, left-side of the histogram).

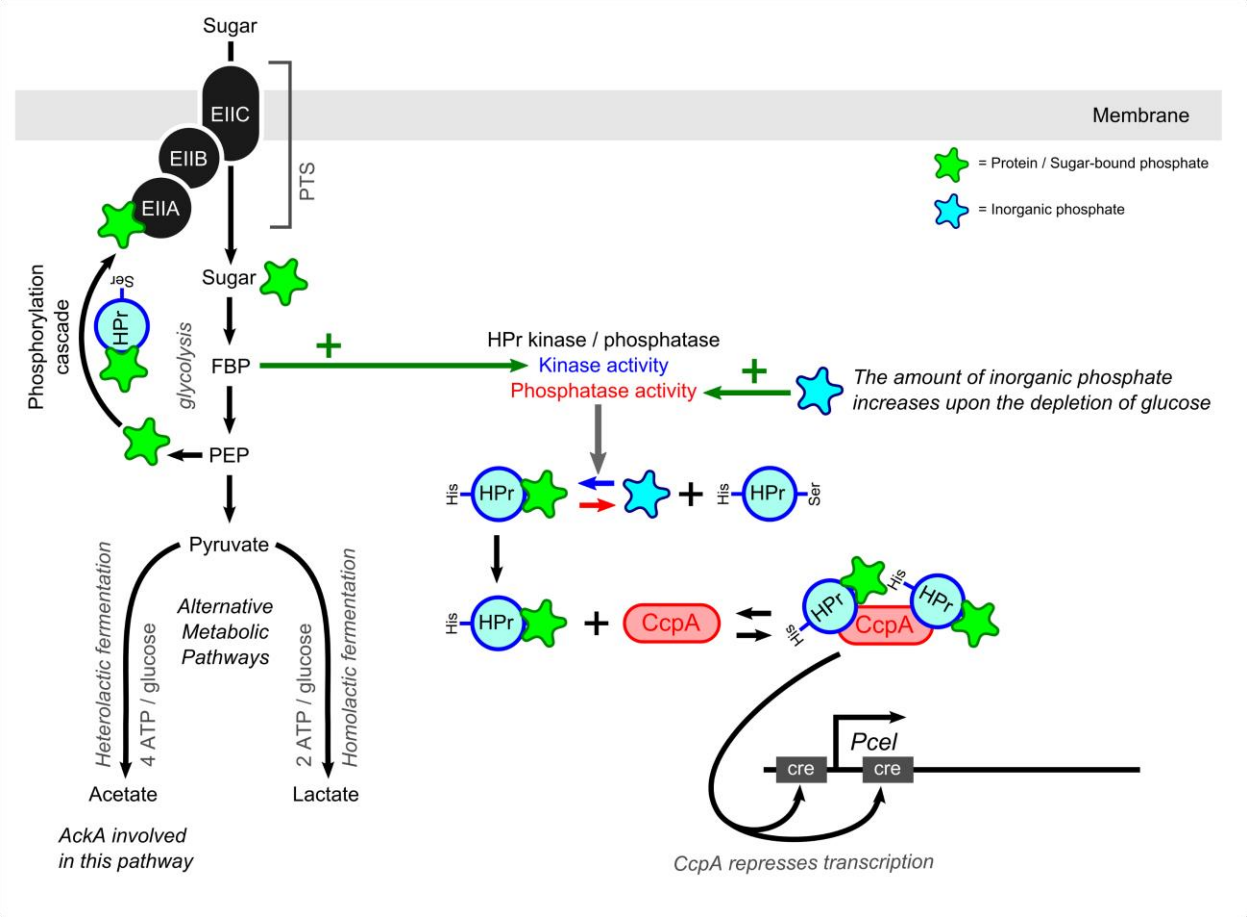

Fig. S5. Intracellular molecular processes during glucose or cellobiose utilization via a phospho-transferase system (PTS) in *L. lactis* M1. Upon uptake of glucose via PTS, it is phosphorylated and directed to glycolysis. The phosphate group is received via a phosphorylation cascade from an intermediate product of glycolysis, phospho-enol-pyruvate (PEP). If the internalized sugar is effectively metabolized and the flux though glycolysis is high (as is the case for glucose metabolism), the cytosolic concentration of fructose 1,6-bisphosphate (FBP) is high. The presence of this compound is sensed by the HPr kinase/phosphatase, and stimulates its kinase activity. HPr kinase/phosphatase phosphorylates HPr at its Ser46 moiety. HPrSer46-P binds to catabolite control protein A (CcpA) and acts as a co-repressor or co-activator of many genes. The promoter of the cellobiose uptake system P*cel* contains two catabolite-responsive elements (*cre*) and is under strong repression of the complex Ccpa-HprSer46-P. The concentration of FBP drops

when the metabolism of the cell (also the flux through glycolysis) slows down (as in case of glucose depletion and cellobiose utilization). The increased amount of inorganic phosphate stimulates the phosphatase activity of HPr kinase/phosphatase. This enzyme then cleaves the phosphate group of HPrSer46-P. Dephosphorylated HPr dissociates from CcpA, leading to DNA-CcpA binding changes. Transcriptional repression of P*cel* is relieved, and the cell starts utilizing cellobiose. The end-products of glycolysis may vary depending on the growth conditions of *L. lactis*. Under optimal conditions of glucose utilization mainly lactate is produced (homolactic fermentation); under less favorable growth conditions (cellobiose utilization), additionally, pyruvate is converted to acetate by acetate kinase (AckA) and to other products (heterolactic fermentation).

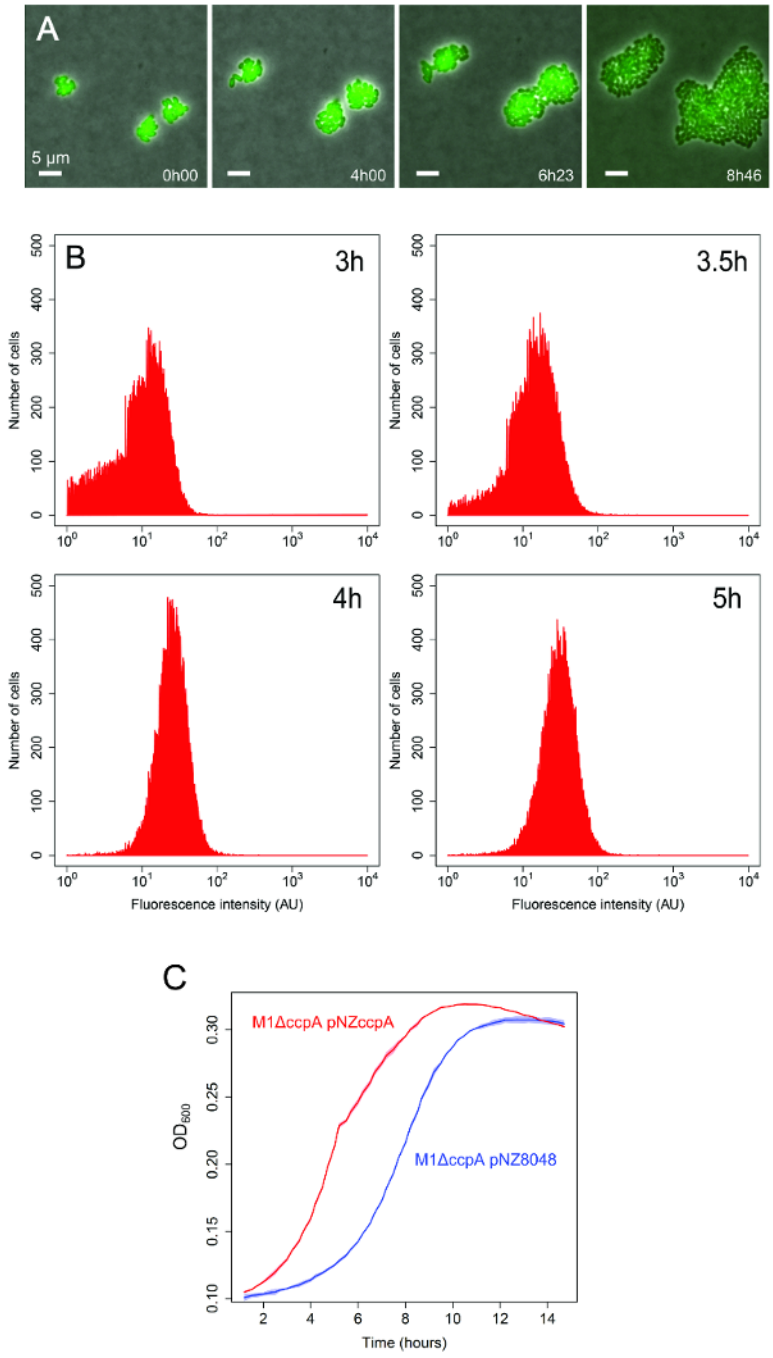

Fig. S6. Deletion of *ccpA* from the chromosome of *L. lactis* M1*gfp* abolishes the heterogeneous expression of the *cel* cluster. (*A*) Snapshots of a time-lapse movie (time indicated in the right lower corner) show that all cells in an *L. lactis* M1*gfp*Δ*ccpA* population simultaneously become fluorescent as soon as they are placed in G-C (0.1%-1%, respectively) medium. (*B*) Fluorescence

of *L. lactis* M1*gfp*Δ*ccpA* cells in G-C medium analyzed at the indicated point in time by flow cytometry. The whole population starts to consume cellobiose and becomes fluorescent immediately after transfer to G-C medium. No diauxie or heterogeneity is observed in this strain. (*C*) Complementation of *ccpA* deletion. Growth of M1Δ*ccpA*pNZ8048 (empty vector; blue line) and that of M1Δ*ccpA*pNZCcpA (complementation strain; red line) in G-C medium (0.15%-1%) with nisin. Expression of *ccpA* from the plasmid restores the wild-type phenotype of M1. Both strains contain a chromosome-integrated *nisRK* for nisin induction. The growth curves show mean and sd (shaded part) for N=2.

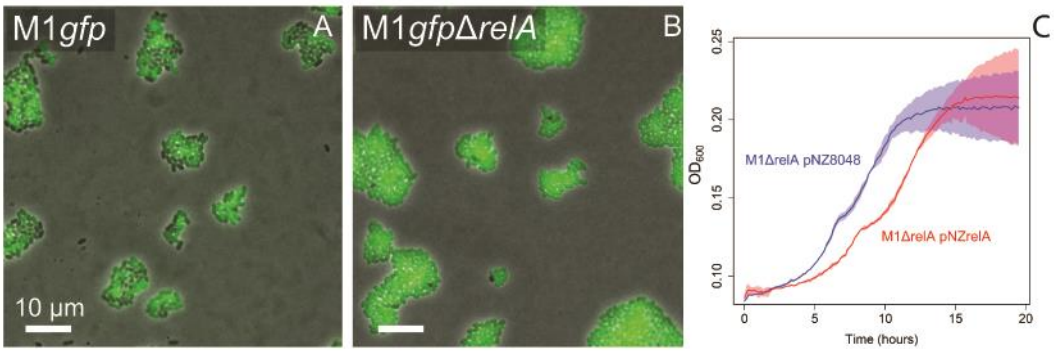

Fig. S7. The fraction of Cel$^+$ cells after the switch point increases in a RelA-deficient (Δ*relA*) derivative of *L. lactis* M1. Microscopy images of a time-lapse experiment (Movie S5) performed on CDM-agarose with glucose (0.1%) and cellobiose (1%). Growth of both strains was monitored simultaneously, under identical conditions. (*A*) M1*gfp* cells are non-fluorescent while growing on glucose. Upon the switch point, a fraction of cells starts to utilize cellobiose and becomes fluorescent (Cel$^+$). Another fraction of cells remains non-fluorescent and stops dividing (Cel$^-$). (*B*) *L. lactis* M1*gfp*Δ*relA* differentiates into two subpopulations upon the switch point like its mother strain. However, the fraction of Cel$^-$ cells in M1*gfp*Δ*relA* is much smaller than the Cel$^-$ fraction of M1*gfp*. (*C*) Complementation of *relA* deletion. Growth of M1Δ*relA*pNZ8048 (empty vector; blue line) and that of M1Δ*relA*pNZ*relA* (complementation strain; red line) in G-C medium (0.15%-1%) with nisin. Both strains contain a chromosome-integrated *nisRK* for nisin induction. The growth curves show mean and sd (shaded part) for N=2.

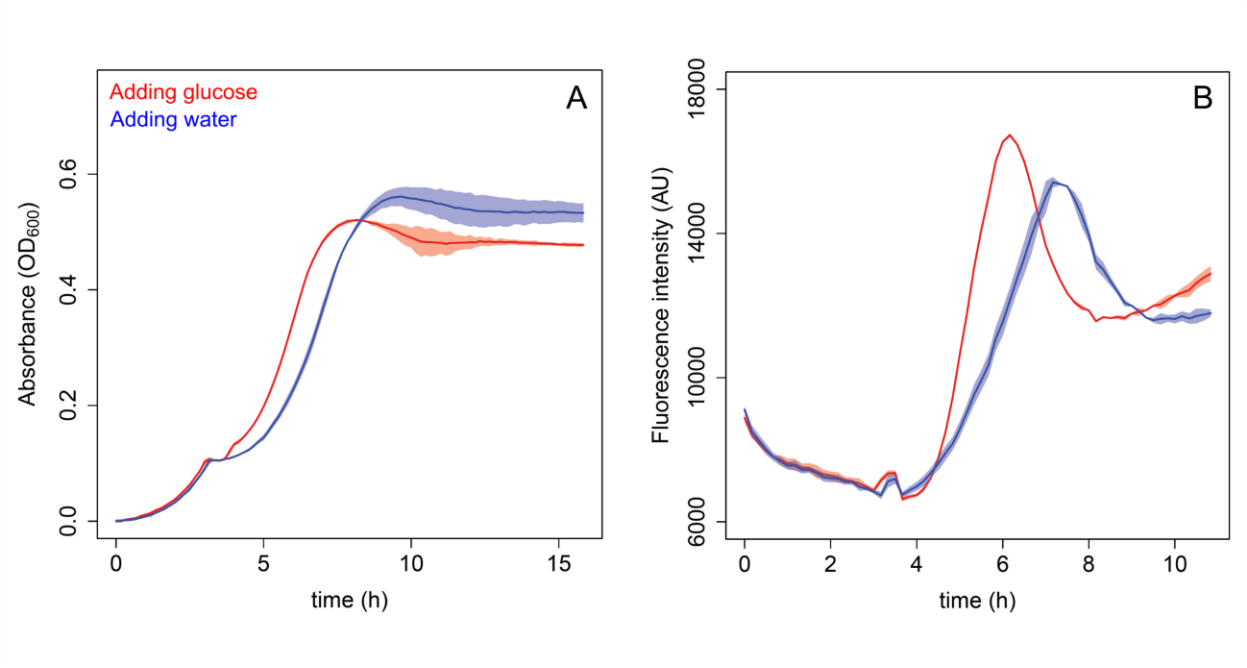

Fig. S8. Addition of glucose shortens the diauxie lag-phase. (*A*) Growth of *L. lactis* M1*gfp* in a medium with glucose (0.1%) and cellobiose (1%). At the diauxie lag-phase, glucose (concentration of 0.01% (w/v): red line) or water (negative control: blue line), was added. The addition of an energy source at the switch point shortened the diauxie lag-phase by increasing the size of the Cel^+ fraction, as indicated by the higher fluorescence intensity peak of the culture to which glucose was added (*B*, red line). Lines show mean ± sd (N=3). The differences in the final OD reached are not caused by differences in available sugar concentrations. The sugar amount in the medium is too high to become growth-limiting. Rather than the sugar, the main growth-stopping factor in *L. lactis* cultures is usually the low pH. *L. lactis* can perform two types of fermentation: homolactic and heterolactic. It is known that the glucose-consuming and fast growing cells mostly produce lactate, therefore, stronger acidify their environment and stop growing at lower OD than those growing slower on a less favorable sugar cellobiose and performing the heterolactic fermentation. Apparently, glucose addition is enough to support and therefore prolong their fast homolactic metabolism prior to the switch to slow cellobiose

utilization. We assume that the acid produced during this short period is enough to make the visible difference in ODs at the end of growth.

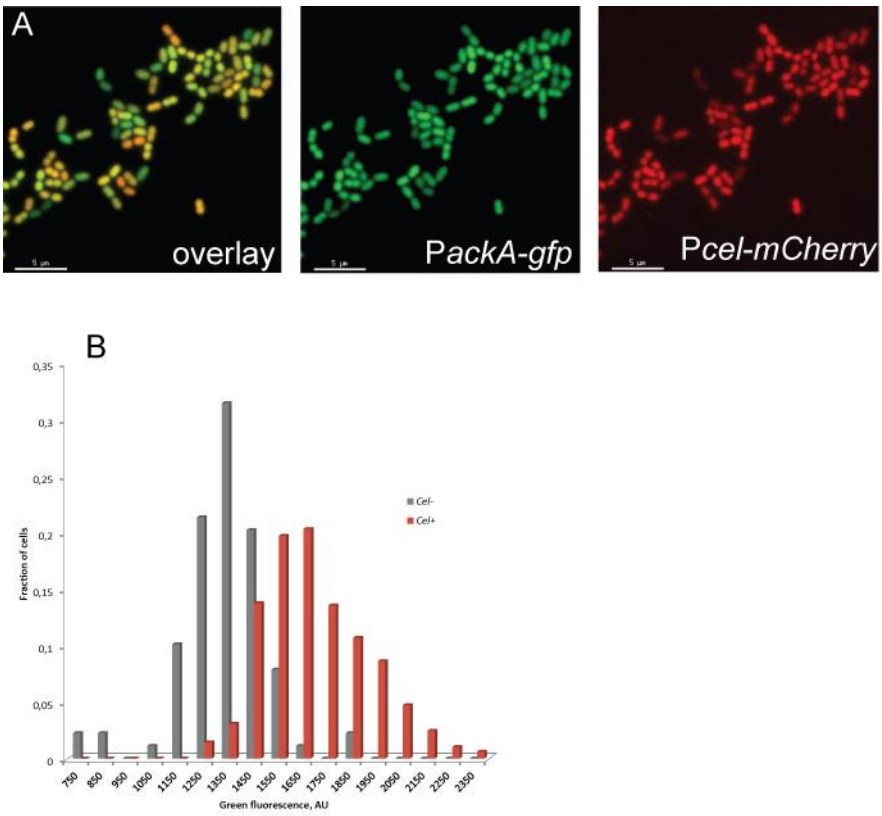

Fig. S9. Expression of acetate kinase AckA and cellobiose transporter IIC component CelB in *L. lactis* M1P*ackA-gfpPcel-mCherry*. Fluorescence was monitored by fluorescence microscopy in G-C medium (1% cellobiose and 0.05% glucose). (*A*) At the diauxie switch the green fluorescence of individual *L. lactis* M1P*ackA-gfp* cells varies; a fraction of cells becomes red-fluorescent (due to *Pcel-mCherry* activity) as the cells switch to cellobiose consumption. (*B*) Comparison of green fluorescence intensity of Cel^+ (red) and Cel^- (non-fluorescent in red channel) cells, calculated from the fluorescence microscopy experiment shown in (*A*). Those cells that are highly green-fluorescent (more P*ackA-gfp*) at the time of glucose exhaustion, are more likely to switch to cellobiose consumption and become red-fluorescent (activity of P*cel-mCherry*) (Mann-Whitney U test: U = 2947.5, p < 2.2e-16, N = 576).

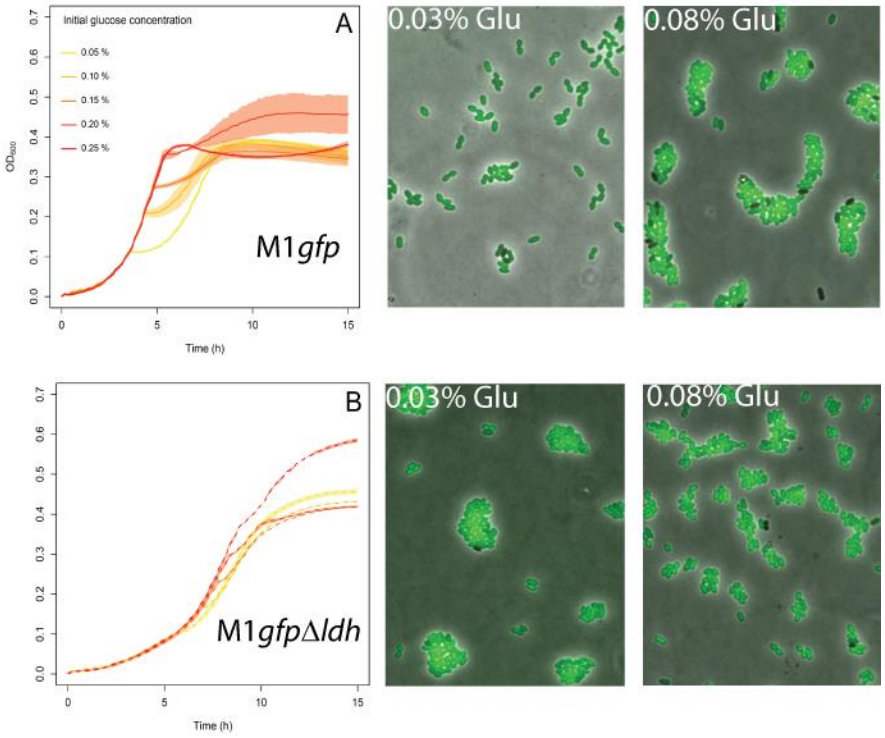

Fig. S10. Deletion of the lactate dehydrogenase (*ldh*) gene of the central enzyme in homolactic fermentation from the chromosome of *L. lactis* M1*gfp* reduces the length of the lag-phase during the diauxic shift from glucose to cellobiose. (*A*) Diauxie of *L. lactis* M1*gfp* in CDM with various concentration of glucose (0.05-0.25%; orange - red) and 1% cellobiose. (*B*) Growth of *L. lactis* M1*gfp*Δ*ldh* under the same conditions as in (*A*). *L. lactis* M1*gfp*Δ*ldh* cells that always perform heterolactic fermentation exhibit a very short diauxie lag-phase as more cells switch to cellobiose consumption and partake in the second growth phase. Fluorescence-microscopy pictures (overlays of phase contrast and green-fluorescence images) of samples from cultures of M1*gfp* and M1*gfp*Δ*ldh* grown in liquid G-C (concentrations are indicated in the upper left corner of each picture) are shown on the right. The growth curves show mean and sd (shaded part) for N=2.

SI Movies:

Movie S1. Glucose-cellobiose diauxie. Time-lapse experiment of *L. lactis* M1*gfp* grown in G-C medium. After glucose is depleted from the medium, two subpopulations emerge. The GFP expression is driven from P*cel* and indicates cellobiose utilization.

Movie S2. Glucose-cellobiose diauxie. Time-lapse experiment of *L. lactis* M1*gfp* grown in G-C medium. After glucose is depleted from the medium, two subpopulations emerge. The GFP expression is driven from P*cel* and indicates cellobiose utilization.

Movie S3. *L. lactis* M1*gfp*Δ*ccpA* in G-C medium. Chromosomal deletion of *ccpA* abolishes the heterogeneous response of *L. lactis* M1Δ*ccpA* to the change in sugar availability.

Movie S4. Cel^- and Cel^+ cells are viable on glucose. Both subpopulations of *L. lactis* M1*gfp* start to divide as soon as they are placed on glucose-containing microscopy slide.

Movie S5. *L. lactis* M1Δ*relA* in G-C medium. Deletion of *relA* from the chromosome of *L. lactis* M1*gfp* increases the fraction of the Cel^+ cells after the switch point.

Movie S6. *L. lactis* M1*gfp* on galactose. Cel^- and Cel^+ subpopulations of *L. lactis* M1*gfp* are not equally fit on galactose-containing medium. Cel^- cells have an advantage in these conditions and divide faster than the Cel^+ cells.

Supporting Information

Solopova et al. 10.1073/pnas.1320063111

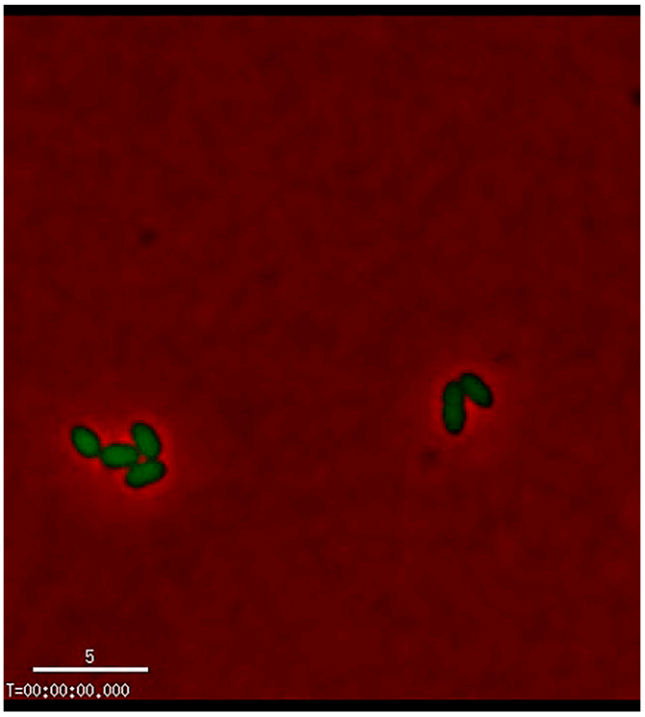

Movie S1. Glucose–cellobiose diauxie. Time-lapse experiment of *Lactococcus lactis* M1*gfp* grown in a medium supplemented with both glucose (0.1%) and cellobiose (1%) (G-C medium). After glucose is depleted from the medium, two subpopulations emerge. The GFP expression is driven from P*cel* and indicates cellobiose utilization.

Movie S1

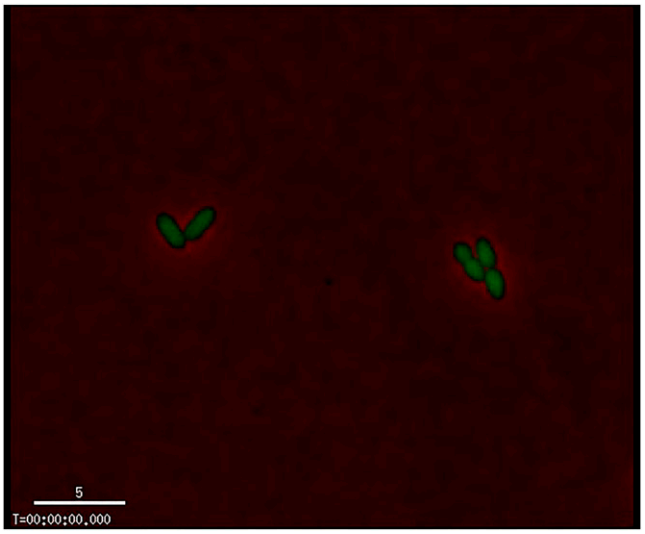

Movie S2. Glucose–cellobiose diauxie. Time-lapse experiment of *L. lactis* M1*gfp* grown in G-C medium. After glucose is depleted from the medium, two subpopulations emerge. The GFP expression is driven from P*cel* and indicates cellobiose utilization.

Movie S2

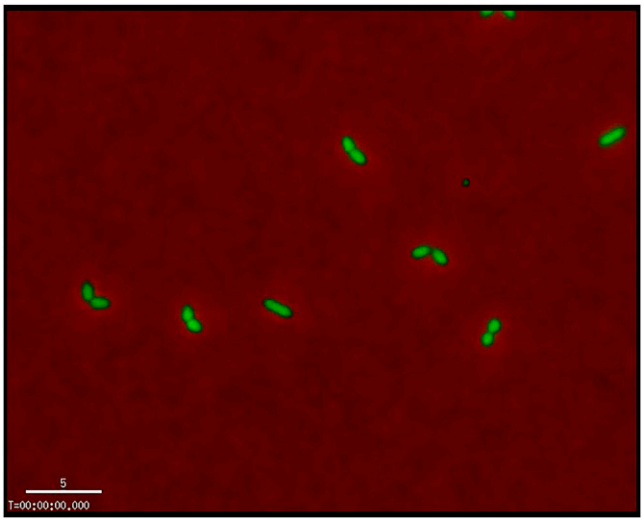

Movie S3. *L. lactis* M1*gfp*Δ*ccpA* in G-C medium. Chromosomal deletion of *ccpA* abolishes the heterogeneous response of *L. lactis* M1Δ*ccpA* to the change in sugar availability.

Movie S3

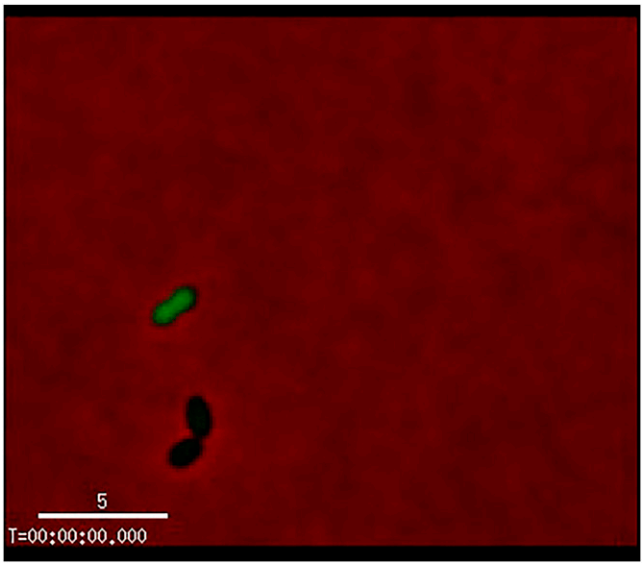

Movie S4. Cel^{-} and Cel^{+} cells are viable on glucose. Both subpopulations of *L. lactis* M1*gfp* start to divide as soon as they are placed on a glucose-containing microscopy slide.

Movie S4

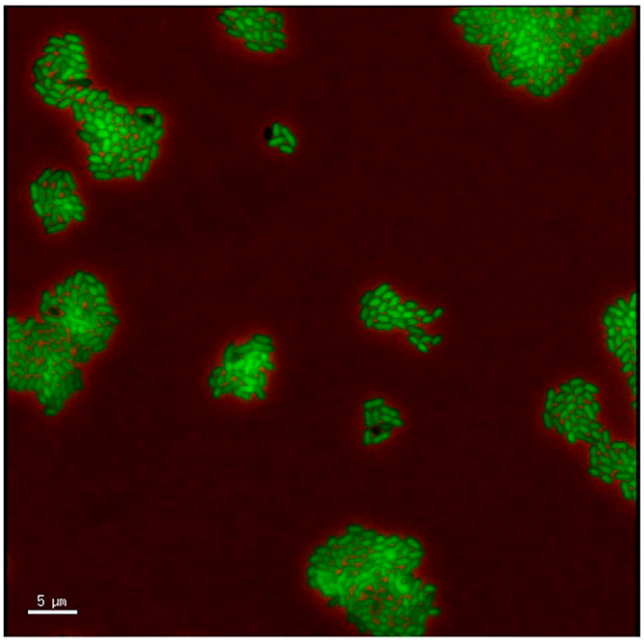

Movie S5. *L. lactis* M1Δ*relA* in G-C medium. Deletion of *relA* from the chromosome of *L. lactis* M1*gfp* increases the fraction of the Cel^+ cells after the switch point.

Movie S5

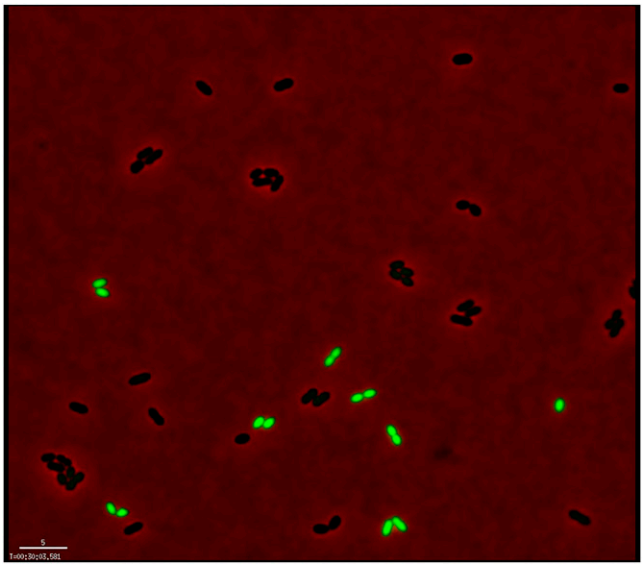

Movie S6. *L. lactis* M1*gfp* on galactose. Cel^- and Cel^+ subpopulations of *L. lactis* M1*gfp* are not equally fit on galactose-containing medium. Cel^- cells have an advantage in these conditions and divide faster than the Cel^+ cells.

Movie S6

Other Supporting Information Files

SI Appendix (PDF)